Polymer Chemistry

Co-initiated hyperbranched-polydendron building blocks for the direct nanoprecipitation of dendron-directed patchy particles with heterogeneous surface functionality

SCHOLARONE™
Manuscripts

Polymer Chemistry is a publication from the Royal Society of Chemistry, encompassing all aspects of synthetic and biological macromolecules, and related emerging areas.

The following paper has been submitted to _Polymer Chemistry_ for consideration as a **Full paper**.

The primary criterion for acceptance of a contribution for publication is that it must report **high-quality** new science and make a significant contribution to its field. Routine or incremental work, however competently researched and reported, should not be recommended for publication. Full papers in _Polymer Chemistry_ should contain original scientific work that has not been published previously. Read more about the scope of _Polymer Chemistry_.

Thank you for your effort in reviewing this submission. It is only through the continued service of referees that we can maintain both the high quality of the publication and the rapid response times to authors.

We would greatly appreciate if you could review this paper in **two weeks**. Please let us know if that will not be possible. Please support all comments with scientific justifications or we may be unable to use your report/ask for extra feedback.

Once again, we appreciate your time in serving as a reviewer. To acknowledge this, the RSC offers referees a **25% discount** on its books. Please also consider submitting your next manuscript to _Polymer Chemistry_.

Best wishes,

Christopher Barner-Kowollik
Editor-in-Chief, _Polymer Chemistry_

UNIVERSITY OF
LIVERPOOL

RSC Publishing
Royal Society of Chemistry

8th March 2018

Steve Rannard BSc DPhil FRSC
Professor of Chemistry

Department of Chemistry
University of Liverpool
Crown Street
Liverpool
L69 7ZD

Telephone: 0044 (0)151 794 3501
Facsimile: 0044 (0)151 794 3588
Email: srannard@liv.ac.uk

Dear Prof. Barner-Kowollik,

Co-initiated hyperbranched-polydendron building blocks for the direct nanoprecipitation of dendron-directed patchy particles with heterogeneous surface functionality.

Thank you very much for rapidly reviewing our manuscript that was recently transferred to *Polymer Chemistry*. The referees have both agreed that the manuscript is acceptable for publication and I am grateful for their time to re-review after initially looking at the manuscript within the context of *Chemical Communications*. Specific comments to their reviews are detailed below:

Referee: 1

"1.   The authors need to discuss the stability of these assembly and cite relevant papers: (Polym. Chem., 2015, 6, 7749–7757, Langmuir 2015, 31, 578−586)."

We have indeed discussed stability in our original submission and included analytical detail of multiple samples after >1 year stored at ambient temperature; this is in the main body of the text and ESI Table S1 where we show no change in size, no obvious colour changes and no precipitation/aggregation.

We have reviewed the papers that are suggested as relevant but we do not see that these reports bare significant resemblance to our work or are, indeed, that relevant. For example: *Polym. Chem., 2015, 6, 7749–7757* reports grafted polyester chains that have undergone ROP from the surface of SiO_2 particles, seeking to use the silica nanoparticle as a surrogate for the core of a polymer micelle. The techniques, rationale, chemistry and targeted outcomes do not relate to our research; *Langmuir 2015, 31, 578−586* describes a strategy for the layer-by-layer (up to 19 layers) deposition of functionalized perylene diimide chromophores on a multivalent porphyrin monolayer which also bears no relevance that we can see to the work that we present.

As such, we have made no changes to the manuscript with respect to this comment from referee 1.

"*2.   Need to rewrite the conclusion in more concisely.*"

We are somewhat at a loss as to how to further summarise our conclusion which was originally written within the constraints of *Chem. Commun.* It is only 1 paragraph long and we see no obvious areas to modify to be more succinct. We would be happy to do this with specific guidance from the Editorial team if they feel that this really is not concise enough but currently have made no changes to the conclusion.

Referee: 2

Has no points that require addressing

I have therefore resubmitted the manuscript without any further changes and I apologise if this does not address the referees' comments adequately. We are just a little lost with respect to knowing what relevant substantive changes can be made given these reviews.

If we can help at all with the further aspects of submission and acceptance for publication, please let me know.

Yours sincerely,

Professor S. P. Rannard

Second cover letter dated 19th February 2018

Dear Editor,

Co-initiated hyperbranched-polydendron building blocks for the direct nanoprecipitation of dendron-directed patchy particles with heterogeneous surface functionality.

We recently submitted the attached manuscript to *Chemical Communications* as article number CC-COM-01-2018-000733 (see cover letter below) and received very positive feedback from two reviewers; however, the submission was considered to be more appropriate for *Polymer Chemistry* and we have gratefully accepted the offer of transfer provided by Dr Alexander Metherell on the 15th of February. Both reviewers are extremely positive about the quality and scope of the research we present and only two minor modifications were requested. Details and full reviews are as follows:

Referee: 1

"*Comments to the Author*

Rannard and co-workers report the synthesis of hyperbranched polydendrons (HPD) via copolymerization of BUMA, EGDMA and functionalized dendrons (G0 and G3). The co-polymers have been efficiently synthesized based on the methodology developed earlier by the group and thoroughly characterized. The number of xanthates (from dendrimer) could be controlled by varying the initiator ratios. The xanthate groups in the HPDs were deprotected and used to obtain nanoparticles (50-70 nm) using the nanoprecipitation method developed earlier by the same group. The exposed thiol groups were used to bind gold nanoparticles to give patchy nanoparticles. This is a very nice and controlled approach for obtaining patchy particles. The area of research is exciting. However, this an extension to the earlier work reported by the authors. The concept of using end functionalized thiols to bind gold nanoparticles has been previously demonstrated by the authors (Ref. 14, Figure 3), though not specifically referred to in the context of patchy particles. The synthesis of almost similar HPDs has been reported earlier by the group (Ref. 12, esp. Polym. Chem. 2017 paper). The current manuscript reports an elegant and detailed study as well as expansion of this previous work. Therefore, I think it is more suitable for publication as a full paper in Polymer Chem. Overall, the experiments have been carried out and explained with care. Some minor issues that can be addressed to improve the paper are:

1. Scheme 1 is very difficult to read. It can probably span the whole page or be suitably modified to improve readability.

2. In the NMR data of compounds, only one J value is given for dd splitting. The second value is missing. In one or two cases a single chemical shift is given for multiplets (instead of a range)."

In response to reviewer 1 we have modified Scheme 1 and have generated a new image that now spans the whole page. This has necessitated the use of the full paper template as the available space within the communication format was not sufficient. In answer to the second point raised, many of the spectra that we have reported actually contain "roofed doublets" and they are not doublets-of-doublets. We have modified the ESI to make this clear by stating the shift for each double resonance and ranges of chemical shifts are now included for all multiplets.

Referee: 2

"*Comments to the Author*

The manuscript of Hern et al. reports a "construction of patchy nanoparticles using hyperbranched-polydendron building blocks'. It is interesting that the rapid construction of patchy nanoparticles from hyperbranched polydendrons containing a controlled mixture of PEG and thiol-functional chain ends. The size of the nanoparticles is characterized by UV-visible spectroscopy and TEM. Since the Author already reported similar assembly of hyperbranched-polydendron into polymer and nanoparticles (Polym. Chem., 2017, 8, 1644 and Chem. Sci., 2014, 5, 1844) and without showing any further applications may not enough to publish in Chemical Communication. The current version is more suitable to be submitted in a specialised organic journal."

There are no suggested modifications required by reviewer 2.

We hope that the changes made to the manuscript and the ESI fully address the comments and that the submission will be acceptable for *Polymer Chemistry*. Please do not hesitate to contact us if you require any additional information

Yours sincerely,

Professor S. P. Rannard

Original cover letter dated 28th January 2018

Dear Editor,

Co-initiated hyperbranched-polydendron building blocks for the direct nanoprecipitation of dendron-directed patchy particles with heterogeneous surface functionality.

We have pioneered a new macromolecular architecture – hyperbranched Polydendrons – in several publications within RSC journals (*Chem. Sci.*, 2014, 5, 1844-1853; *Chem. Sci.*, 2015, 6, 326-334; *Soft Matter*, 2015,11, 7005-7015; *Chem. Commun.*, 2016, 52, 3915-3918; *Polym. Chem.* 2017,8, 1644-1653) including the concept of highly branched linear-dendritic hybrid polymers. These materials offer large benefits over dendrimers as their synthesis is fast and scalable and they possess the multi-valency aspects of ideal dendrimers. Importantly, these materials nanoprecipitate to form very uniform polymer nanoparticles, despite their highly disperse polymer distributions leading to considerable interest. Here, we present a detailed report of a new potential benefit for hyperbranched Polydendrons – mixed initiation to generate spatially zoned chemistry capable of generating patchy nanoparticles. We have approached this highly active field through a "design of building block" approach that controls chain-end functionality and, for the first time, created evidence of zoned thiol "patches" at the surface of nanoprecipitates.

Nanoprecipitation is known to undergo a nucleation and growth mechanism during the solvent switch process. Very few reports exist that utilise the benefits of complex architectures in this process and fewer exist that attempt to use the architecture to control surface functionality. Here, we directly compare the single functional groups at the chain-ends of conjoined complex architectures with grouped dendron-containing materials with similar molecular weight, numbers of thiols (grouped or isolated) and additional PEG chains for stabilisation of nanoparticles. We have used the binding of gold nanoparticles to visualise the "patchiness" and establish the different distribution of surface clusters. We believe there are many aspects of novelty within this report, not just for our complex polymer architectures, but in the field of nanoprecipitation and the formation of heterogeneously functionalised nanoparticles. We also supply over 30 pages of supporting information including synthetic, experimental, spectroscopic, chromatographic and nanoparticle characterisation information.

Due to the considerable interest in approaches to polymer nanoparticle formation, and the global debate and interest in patchy particles, an increasing interest in polymer architectures, the growth of studies of nanoprecpitation and the use of nanoprecipitates within novel drug delivery applications, we believe that this report will be of great interest to academic and industrial scientists. Scientists from a wide spectrum of disciplines including materials science, life sciences, pharmaceutical development, pharmacy, colloids, and polymers will identify aspects of the report that may impact their research, especially those focused at the interfaces between nanotechnology, materials and medicine.

We have not published any previous papers regarding this work and we strongly believe that *Chemical Communications* will provide the broad exposure required to disseminate rapidly the benefits of this chemistry to a wide audience.

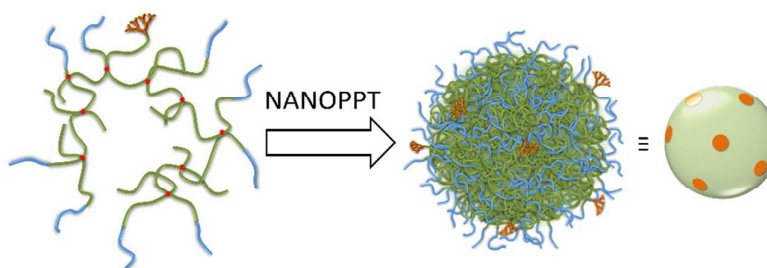Please do not hesitate to contact us if you require any additional information

Yours sincerely,

Professor S. P. Rannard

Graphical Abstract

Co-initiated hyperbranched-polydendron building blocks for the direct nanoprecipitation of dendron-directed patchy particles with heterogeneous surface functionality

F. Y. Hern, A. Hill, A. Owen and S. P. Rannard*

A synthetic strategy for generating branched polymer building blocks for the rapid construction of patchy nanoparticles is presented. Hyperbranched polydendrons containing a controlled mixture of PEG and thiol-functional chain ends, with different dendron generation (G0 and G3), were synthesised and nanoprecipitated (50-70 nm). The patchy isolation of thiol groups was confirmed through the binding of 4 nm gold particles and the quantification of clustering at the nanoprecipitate surface.

Journal Name

ARTICLE

Co-initiated hyperbranched-polydendron building blocks for the direct nanoprecipitation of dendron-directed patchy particles with heterogeneous surface functionality

F. Y. Hern[a], A. Hill,[a] A. Owen[b] and S. P. Rannard*[a]

A synthetic strategy for generating branched polymer building blocks for the rapid construction of patchy nanoparticles is presented. Hyperbranched polydendrons containing a controlled mixture of PEG and thiol-functional chain ends, with different dendron generation (G_0 and G_3), were synthesised and nanoprecipitated (50-70 nm). The patchy isolation of thiol groups was confirmed through the binding of 4 nm gold particles and the quantification of clustering at the nanoprecipitate surface.

Introduction

Colloidal and nano-particles with surface anisotropy, known widely as "patches", have been created using a range of techniques that are largely process-driven, using masking or templated mechanisms, and often employing a mixture of inorganic and organic structures.[1] These novel materials have undergone various studies of their behaviour including interactions at liquid-liquid interfaces[2], with biological molecules such as proteins[3] and self-assembly.[4] Recently, manipulation of solvent quality has been used to impact the nanoprecipitation of mixed homogeneous solutions of glassy/non-glassy phase-separating polymers[5] and the solvation of macromolecules to create pinned micelles on spherical gold nanoparticles.[6]

Nanoprecipitation has been applied to a range of homopolymers and block copolymers and is a highly efficient polymer nanoparticle synthesis.[7] Our studies of lightly branched vinyl polymers has shown that polymer architecture can strongly influence rapid nanoprecipitation[8] and co-nanoprecipitation outcomes including particle size, stability, and organic/inorganic magnetic nanocomposite formation.[9] This understanding led to the formation of uniform functional nanoprecipitates from dendron-initiated branched copolymers, termed hyperbranched-polydendrons (HPDs), under organic/organic and organic/aqueous (neutral and varying pH) precipitation conditions.[10] HPDs may be synthesised *via* co-initiation, creating conjoined chains with a mixture of chain-end

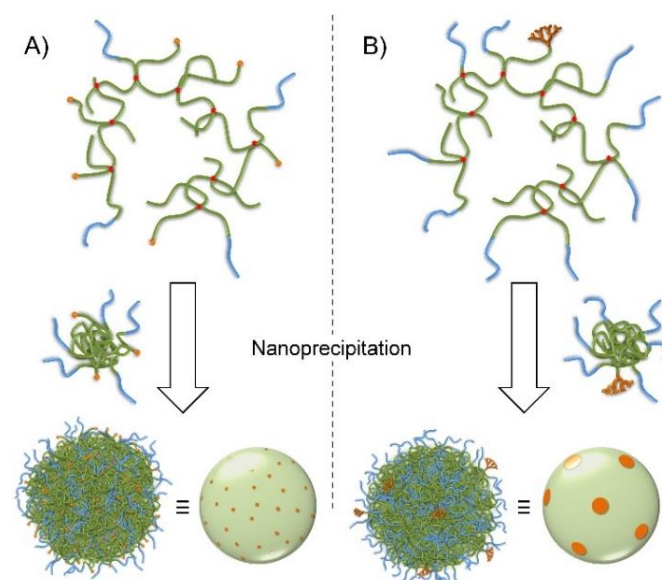chemistry, Fig. 1, and subsequent control of nanoprecipitate internal environment and surface functionality.[11]

Fig. 1 Strategy for patchy particle formation from co-initiated HPDs using PEG initiators and either A) single-functional G_0 or B) eight-functional G_3 dendrons

We hypothesised that co-initiation of hydrophobic HPDs with a mixture of functional dendron and poly(ethylene glycol) (PEG) initiators would allow isolation of surface functionality after nanoprecipitation and the subsequent formation of "patchy" particles, Fig. 1. By targeting G_0 (Fig. 1A & 2A) and G_3 (Fig. 1B & 2B) dendrons bearing either one or eight functional groups respectively, and varying the molar dendron:PEG initiator ratio, HPDs comprising identical numbers of functional groups could be generated that would create nanoparticles with spatially-controlled or statistically distributed surface groups.

a. Department of Chemistry, University of Liverpool, Crown Street, L69 7ZD, UK.
b. Department of Molecular and Clinical Pharmacology, University of Liverpool, Block H, 70 Pembroke Place, Liverpool L69 3GF, U.K.
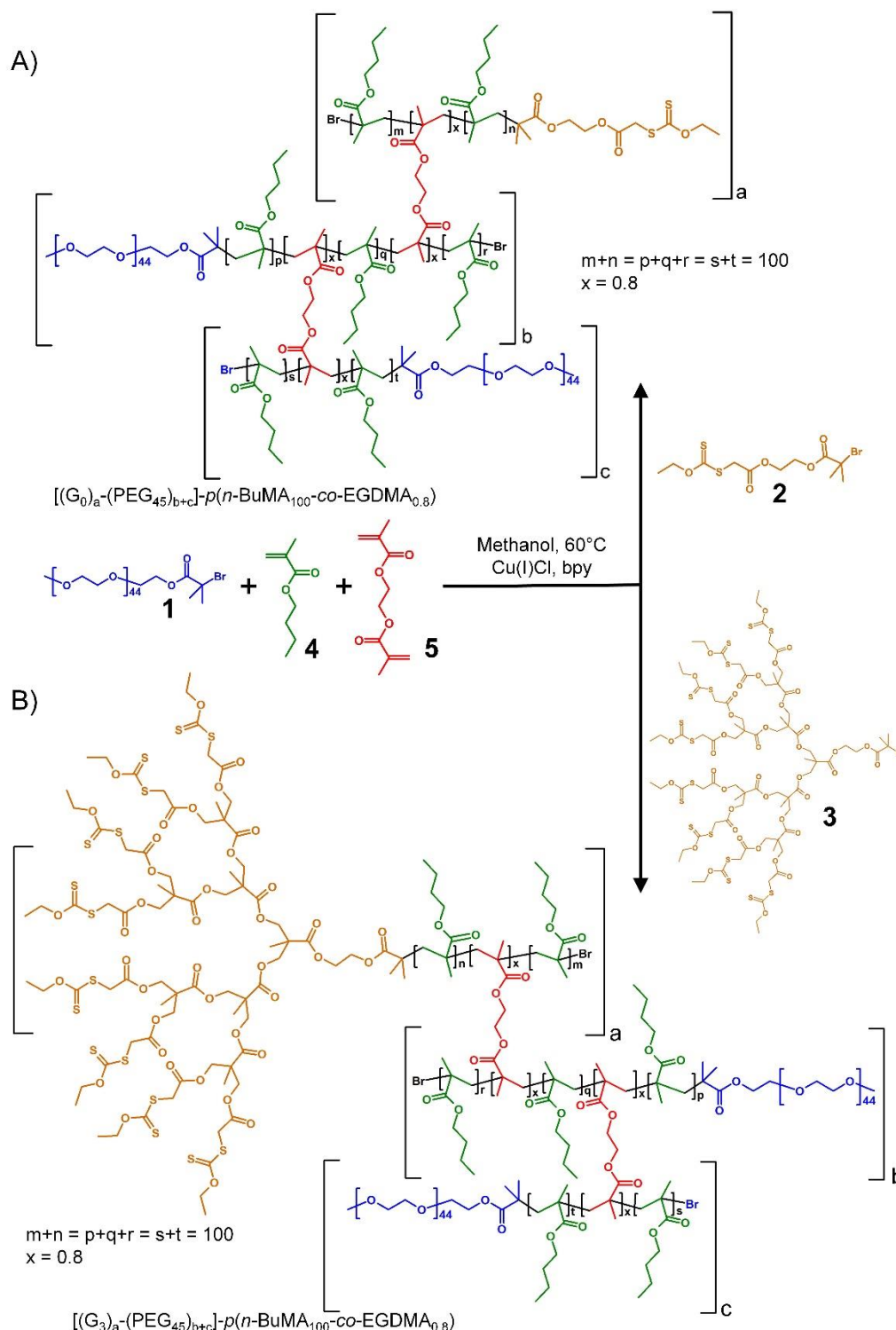*E-mail: srannard@liverpool.ac.uk

Results and Discussion

The HPDs studied here were synthesised using methanolic copper-catalysed atom transfer radical polymerisation (ATRP) strategies that we have previously reported; initiated with combinations of a monomethyl-PEG$_{45}$ initiator (number average molecular weight (M_n) approx. 2000 g mol^{-1}), **1**, with either G$_0$, **2**, or G$_3$, **3**, xanthate-functional polyester dendron initiators described previously,[12] Scheme 1 (ESI Figs S1-48).

$m+n = p+q+r = s+t = 100$
$x = 0.8$

$[(G_0)_a\text{-}(PEG_{45})_{b+c}]\text{-}p(n\text{-}BuMA_{100}\text{-}co\text{-}EGDMA_{0.8})$

Methanol, 60°C
Cu(I)Cl, bpy

$m+n = p+q+r = s+t = 100$
$x = 0.8$

$[(G_3)_a\text{-}(PEG_{45})_{b+c}]\text{-}p(n\text{-}BuMA_{100}\text{-}co\text{-}EGDMA_{0.8})$

Scheme 1 Co-initiation of methanolic atom transfer radical copolymerisation of *n*-butyl methacrylate/ethylene glycol dimethacrylate to form hyperbranched-polydendrons. Initiator compositions are A) monomethyl-PEG$_{45}$-Br/G$_0$-xanthate functional initiator, or B) monomethyl-PEG$_{45}$-Br/G$_3$-xanthate functional initiator

The hydrophobic monomer *n*-butyl methacrylate (*n*-BuMA; **4**) was selected for the primary chains of the HPDs with branching achieved by the addition of a low molar concentration (< 1 per chain) of ethylene glycol dimethacrylate (EGDMA; **5**). We have

previously shown the high level of control within methanolic ATRP (60°C) of n-BuMA;[13] however, the primary chain structures formed during HPD synthesis – namely a linear dendritic hybrid, a xanthate-functional homopolymer and the amphiphilic A-B block copolymer p(PEG$_{45}$-b-n-BuMA$_{100}$) – were all synthesised individually to ensure the conditions (CuCl:bpy (1:2); 50 v/v% wrt. monomer) were appropriate for the envisaged strategy, Table 1; the HPD synthesis effectively joins combinations of these diverse polymer structures together into complex branched structures, Scheme 1.

Table 1 SEC characterisation of linear polymers and hyperbranched-polydendrons (HPDs)

Target Polymer (HPD = X- $p(n$-BuMA$_{100}$-co-EGDMA$_{0.8}$))	Conv.[a] (%)	SEC[b] M_n (g mol^{-1})	M_w (g mol^{-1})	Đ	Thiol (%)[d]
Linear polymers					
G$_0$-$p(n$-BuMA)$_{100}$	95	21700	26400	1.21	-
G$_3$-$p(n$-BuMA)$_{100}$	84	26600	31800	1.19	-
p(PEG$_{45}$-b-n-BuMA$_{100}$)	94	13400	14500	1.08	-
HPDs					
[(G$_0$)$_{0.01}$-(PEG$_{45}$)$_{0.99}$]-HPD	99	43100	283000	6.56	1
[(G$_0$)$_{0.075}$-(PEG$_{45}$)$_{0.925}$]- HPD	94	36400	216200	5.94	7.5
[(G$_0$)$_{0.1}$-(PEG$_{45}$)$_{0.9}$]- HPD	98	41600[c]	149600[c]	3.60[c]	10
[(G$_3$)$_{0.01}$-(PEG$_{45}$)$_{0.99}$]- HPD	97	39200	235700	6.01	7.5
[(G$_3$)$_{0.014}$-(PEG$_{45}$)$_{0.986}$]- HPD	99	39900[c]	185700[c]	4.66[c]	10
[(G$_3$)$_{0.05}$-(PEG$_{45}$)$_{0.95}$]- HPD	98	37200	190400	5.12	30

[a]Determined by ^{1}H NMR analysis in CDCl$_3$, reactions terminated after 21-28 hours; [b]DMF eluent containing 0.01 M LiBr at 60°C, 1mL min^{-1}; [c] THF eluent containing 2% TEA (v/v) at 35°C, 1mL min^{-1}; [d]mole % thiol relative to total chain ends present

Polymerisations of the individual linear primary chains, Table 1, yielded low dispersity (Đ) samples with high conversions after 21-28 hours. Both G$_0$ and G$_3$ initiators showed reduced initiator efficiencies with near-linear semi-logarithmic and evolution of M_n vs. conversion plots as previously reported (ESI Fig S43).

The synthesis of HPDs, co-initiated with varying **1:2** or **1:3** ratios, and incorporating an EGDMA:total initiator molar ratio of 0.8:1, yielded six branched polymers with similar M_n and weight average molecular weight (M_w) values, Đ values ranging between 3.6 – 6.6, Table 1. By varying the co-initiation ratio, the average number of xanthates relative to PEG chains was controlled across the complex architectures and nuclear magnetic resonance (NMR) analysis was utilised to confirm the expected ratios of chain ends in the final purified samples. M_w provides an indication of the polymer structures that contribute the majority of the physical mass of the sample and by dividing the M_w of each HPD by an averaged value of the component linear polymers, the number of conjoined chains in these macromolecules can be estimated. The HPDs co-initiated with **2**, therefore, can be estimated as having 14, 11 and 7 chains (weight average number) as the mole % of **2** increases from 1% through to 10%; similarly, increasing **3** in the co-initiation mixture leads to an estimated weight average number of chains from 10 to 8; the number average number of conjoined chains is consistent at approximately 2 across all samples. Size exclusion chromatography (SEC) of the polymers suggests structures with considerably higher numbers of conjoined

chains are also present with molecular weights that extend >10^6 g mol^{-1} (ESI Figs S51-59). A clear implication of the estimated number of chains (weight and number average) is that many polymers have very few or no xanthate functional groups, at the **1:2** and **1:3** ratios used here, and the functional groups will be widely distributed across the macromolecules within each sample. The initiator ratios were selected to achieve this, as nanoprecipitation is hypothesised to create a spatial surface distribution derived from this chemical inhomogeneity. The xanthates here act as protected thiol groups with deprotection achieved by addition of a molar excess of n-butylamine, as confirmed by NMR studies (ESI Figs S49-50). Each G$_3$ dendron carries eight thiol chain-ends; therefore, the thiol mole % relative to total chain-ends varies from 7.5 to 30% within the G$_3$ co-initiated samples, and from 1 to 10% for G$_0$ co-initiated HPDs, Table 1. As such, materials with a near-identical thiol mole % have been achieved using either **2** or **3**, but the specific number of PEG chains per polymer sample is considerably higher for HPDs derived from **3** in these samples.

Nanoprecipitation via the rapid addition of a thiol-functional HPD acetone solution (2 mL; 5 mg mL^{-1}) into stirred deionised water (10 mL) was employed. The nanoparticle dispersions were left stirring at ambient temperature overnight to allow acetone evaporation, leaving a final 1 mg mL^{-1} nanoparticle concentration after replacement of co-evaporated water. The six unfiltered dispersions were analysed by dynamic light scattering (DLS) and particle distributions with z-average diameters (D_z) ranging from 52-65 nm with narrow polydispersities (0.083 – 0.141) were observed, Table 2.

Table 2 Dynamic light scattering analysis of nanoprecipitated thiol-functional polymers

HPD = X-$p(n$-BuMA$_{100}$-co-EGDMA$_{0.8}$) Co-initiation composition	Gold nanoparticles (4 nm; +/-)	D_z (nm)	PDI
[(SH$_1$ G$_0$)$_{0.01}$-(PEG$_{45}$)$_{0.99}$]-HPD	-	53	0.128
[(SH$_1$ G$_0$)$_{0.01}$-(PEG$_{45}$)$_{0.99}$]-HPD	+	60	0.230
[(SH$_1$ G$_0$)$_{0.075}$-(PEG$_{45}$)$_{0.925}$]-HPD	-	52	0.083
[(SH$_1$ G$_0$)$_{0.075}$-(PEG$_{45}$)$_{0.925}$]-HPD	+	64	0.224
[(SH$_1$ G$_0$)$_{0.1}$-(PEG$_{45}$)$_{0.9}$]-HPD	-	65	0.097
[(SH$_1$ G$_0$)$_{0.1}$-(PEG$_{45}$)$_{0.9}$]-HPD	+	74	0.235
[(SH$_8$ G$_3$)$_{0.01}$-(PEG$_{45}$)$_{0.99}$]-HPD	-	51	0.105
[(SH$_8$ G$_3$)$_{0.01}$-(PEG$_{45}$)$_{0.99}$]-HPD	+	54	0.124
[(SH$_8$ G$_3$)$_{0.014}$-(PEG$_{45}$)$_{0.986}$]-HPD	-	61	0.141
[(SH$_8$ G$_3$)$_{0.014}$-(PEG$_{45}$)$_{0.986}$]-HPD	+	66	0.190
[(SH$_8$ G$_3$)$_{0.05}$-(PEG$_{45}$)$_{0.95}$]-HPD	-	52	0.101
[(SH$_8$ G$_3$)$_{0.05}$-(PEG$_{45}$)$_{0.95}$]-HPD	+	56	0.101

In previous unrelated work, we confirmed the cleavage of disulphide bonds in shaped polymer nanoparticles through gold nanoparticle (GNP) binding and transmission electron microscopy (TEM) of diluted samples.[14] Here, we hypothesised that small GNPs would also bind with the deprotected thiols on the PEG-stabilised nanoprecipitate surfaces and potentially allow imaging of the patchy or statistical-nature of the presentation of thiols. The inverse Turkevich method was employed to synthesise citrate/tannic acid stabilised 4 nm mean diameter spherical GNPs, with confirmation of success obtained by UV-visible spectroscopy and TEM (ESI Figs S60-61).

GNP binding to the aqueous thiol-functional HPD nanoprecipitates was readily observed visually with the formation of transparent red dispersions without obvious aggregation, agglomeration or macro-precipitation (ESI Table S1). DLS studies of the samples with bound GNPs showed larger D_z values in all cases, ranging from increases in diameter between 7-12nm for G_0-initated materials and 3-5 nm for G_3-initiated HPD nanoprecipitates, Table 2); these dispersions were stable for >1 year at ambient temperature (ESI Table S1). Computational estimates of the thiol-functional G_3 dendron, using the Avogadro molecule editor (v1.2.0), suggests a distance of approximately 2.3 nm across the dendron width and approximately 1.3 nm across the G_3 dendron segment, Fig. 2A.
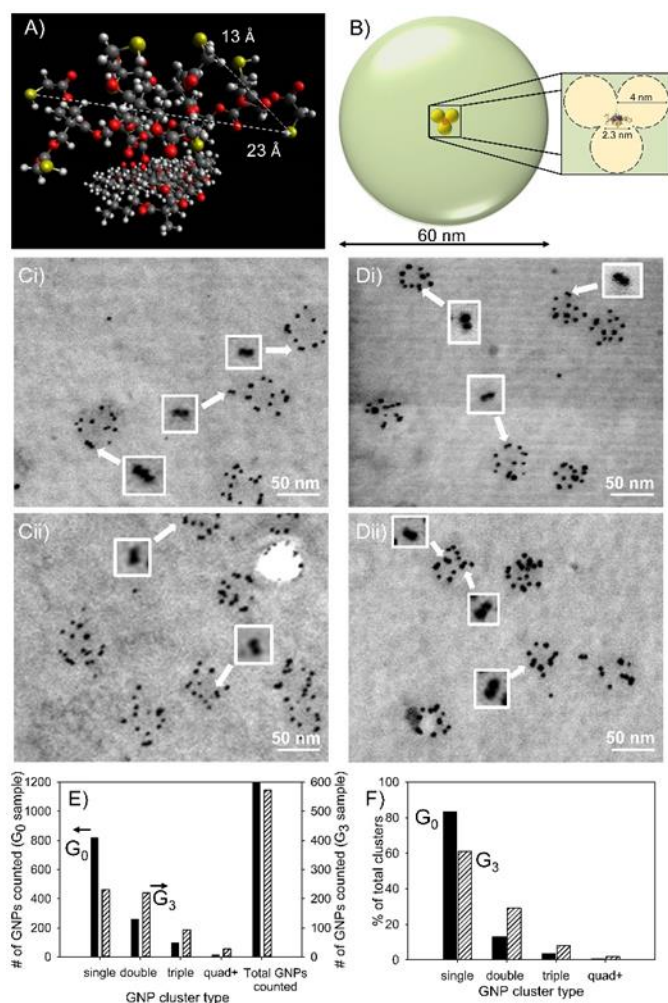

Fig. 2 Thiol-functionality "patchiness" studies. A) Size approximations of the G_3 thiol-functional dendron; B) Schematic representation of a 60nm nanoprecipitate with 4 nm gold nanoparticles (GNPs) and the G_3 thiol-functional dendron; Ci-ii) TEM imaging of surface clustered GNPs on nanoprecipitates of $[(G_0)_{0.1}-(PEG_{45})_{0.9}]$-$p(n$-BuMA$_{100}$-$co$-EGDMA$_{0.8}$); Di-ii) TEM imaging of clustered GNPs on the surface of nanoprecipitates of $[(G_3)_{0.014}-(PEG_{45})_{0.986}]$-$p(n$-BuMA$_{100}$-$co$-EGDMA$_{0.8}$); E) Analysis of spatial arrangement of individual GNPs within the TEM analysis of G_0-(solid bars) and G_3-derived (hashed bars) nanoprecipitates; F) Analysis of GNP cluster type by percentage of all clusters within the TEM analysis of G_0- (solid bars) and G_3-derived (hashed bars) nanoprecipitates.

When considered in proportion to a 60 nm nanoprecipitate, it is theoretically possible that up to three 4 nm GNPs could bind

to a thiol-functional G_3 surface dendron, Fig, 2B, generating an observable GNP cluster; clearly, a single GNP may also bind to a G_3 dendron, obscuring access for other GNPs; single thiols from the G_0 dendron would be expected to bind just one GNP. Statistically, it is reasonable to assume each dendron type may individually appear in close proximity, also leading to observable GNP clustering; such clustering being more likely for G_0-derived thiols as there are 8 G_0 chain-ends for each G_3 dendron for all compositions matching thiol numbers, Table 1. TEM studies of nanoprecipitates-bound GNPs (matching thiol numbers), Fig. 2, allowed quantification of the different sized clusters; GNPs were considered clustered if ≥two particles were visibly touching. In all samples, isolated single GNPs were the most common species, but higher order clusters (≥two GNPs) were frequently seen, Fig. 2 C&D. Quantification of the number of clusters, containing one to ≥four GNPs, within samples derived from $[(G_0)_{0.1}-(PEG_{45})_{0.9}]$-$p(n$-BuMA$_{100}$-$co$-EGDMA$_{0.8}$) and $[(G_3)_{0.014}-(PEG_{45})_{0.986}]$-$p(n$-BuMA$_{100}$-$co$-EGDMA$_{0.8}$) comprising a nominal 10 mole % thiol functionality relative to total chain-ends, showed a considerable bias towards clusters of ≥two GNPs within G_3-initiated materials, Fig. 2 E&F.

For the G_0-initiated samples, 1193 individual GNPs were observed as either single isolated GNPs (820; 68.7%) or clusters containing two GNPs (258 total; 21.6%), three GNPs (99 total; 8.3%) or ≥four GNPs (16 total; 1.3%), Fig. 2E. Similar observation of 572 individual GNPs within the G_3-initiated samples showed a markedly different distribution; 231 single GNPS (40.4%), 220 GNPs as double clusters (38.5%), 93 GNPs as triple clusters (16.3%) and 28 GNPs in clusters ≥four GNPs (4.9%), Fig. 2E. This strongly suggests that GNPs were near-equally likely to be part of a clustered pair on G_3-containing nanoprecipitates as they were to be isolated as single GNPs; in comparison, individual GNPs were less than a third as likely to be in a clustered pairing than isolated within the G_0-containing nanoprecipitates. Similarly, GNPs were nearly twice as likely to gather into triple clusters, and >3.5 times as likely be in clusters of ≥four GNPs within the G_3-samples relative to G_0-derived nanoprecipitates.

An alternative quantification approach treats each cluster as a single entity, normalising the percentage of single GNPs and cluster type in each sample, Fig. 2F. Using this approach, a total of 986 GNP-derived entities were seen in the G_0-samples and 379 entities in the G_3-samples. Analysis of the G_0-derived samples showed 820 isolated single GNPs (83.2%) amongst a distribution of 129 clusters of two GNPs (13.1%), 33 clusters with three GNPs (3.3%) and 4 clusters with ≥four GNPs (0.4%); corresponding G_3-derived sample figures are 231 single GNPs (60.9%), 110 clusters of two GNPs (29%), 31 clusters containing three GNPs (8.2%) and 7 clusters with ≥four GNPs (1.8%), Fig. 2F. Despite larger numbers of thiol-bearing chain-ends in the G_0-derived nanoprecipitates, the G_3 dendrons appear to impact GNP clustering, presumably due to the additional dendron-directed anisotropic spatial distribution of thiol functionality.

Conclusions

When considering the normalised percentage distribution of entities, Fig. 2E, the prevalence of single GNPs at G_0-derived

nanoprecipitate surfaces (almost 1.4-fold higher than G_3-derived materials), and the increased likelihood of higher order GNP clusters at the surface of G_3-initiated HPD nanoprecipitates (two GNPs = 2.2-fold; three GNPs = 2.4-fold; ≥four GNPs = 4.5-fold) is compelling evidence to suggest that the creation of patchy surfaces can be "designed-into" the initial branched copolymer building blocks of polymer nanoprecipitates. Importantly, the same procedures were employed for nanoprecipitation of the G_0 and G_3-initiated HPDs, demonstrating that patch formation is not process-driven but directed by the different multiplicity of thiols within the chain-end generations. This novel strategy may offer benefits to creating functional patchy nanoparticles for a range of applications and we are actively pursuing this area of research.

Conflicts of interest

SR, FH and AO are co-inventors of patents related to HPDs.

References

1   J. Du and R. K. O'Reilly, *Chem. Soc. Rev.*, 2011, **40**, 2402; A. Walther and A. H. E. Müller, *Chem. Rev.*, 2013, **113**, 5194; E. Bianchi, P. D. J. van Oostrum, C. N. Likos and G. Kahl, *Current Opin. Colloid In.*, 2017, **30,** 8.
2   L. C. Bradley, W-H. Chen, K. J. Stebe and D. Lee, *Current Opin. Colloid In.*, 2017, **30,** 25.
3   W. Fan, L. Liu and H. Zhao, *Angew. Chem.*, 2017, **56**, 8844.
4   G-R. Yi, D. J. Pine and S. Sacanna, *J. Phys. Condens. Matter*, 2013, **25**, 193101; D. J. Lunn, J. R. Finnegan and I. Manners, *Chem. Sci.*, 2015, **6**, 3663.
5   C. Sosa, V. E. Lee, L. S. Grundy, M. J Burroughs, R. Liu, R. K. Prud'homme and R. D. Priestley, *Langmuir* 2017, **33**, 5835.
6   R. M. Choueiri, E. Galati, H. Thérien-Aubin, A. Klinkova, E. M. Larin, A. Querejeta-Fernández, L. Han, H. L. Xin, O. Gang, E. B. Zhulina, M. Rubinstein and E. Kumacheva, *Nature*, 2016, **538**, 79.
7   W. S. Saad and R. K. Prud'homme, *Nano Today*, 2016, **11**, 212.
8   R. A. Slater, T. O. McDonald, D. J. Adams, E. R. Draper, J. V. M. Weaver and S. P. Rannard, *Soft Matter*, 2012, **8**, 9816; J. Ford, P. Chambon, J. North, F. L. Hatton, M. Giardiello, A. Owen and S. P. Rannard, *Macromolecules*, 2015, **48**, 1883; F. L. Hatton, P. Chambon, A. C. Savage and S. P. Rannard, *Chem. Commun.*, 2016, **52**, 3915.
9   M. Giardiello, F. L. Hatton, R. A. Slater, P. Chambon, J. North, A. K. Peacock, T. He, T. O. McDonald, A. Owen and S. P. Rannard, *Nanoscale*, 2016, **8**, 7224.
10 F. L. Hatton, P. Chambon, T. O. McDonald, A Owen and S. P. Rannard, *Chem. Sci.*, 2014, **5**, 1844; H. E. Rogers, P. Chambon, S. E. R. Auty, F. Y. Hern, A. Owen and S. P. Rannard, *Soft Matter*, 2015, **11**, 7005.
11 F. L. Hatton, L. M. Tatham, L. R. Tidbury, P. Chambon, T. He, A. Owen and S. P. Rannard, *Chem. Sci.*, 2015, **6**, 326.
12 S. E. R. Auty, O. Andrén, M. Malkoch and S. P. Rannard, *Chem. Commun.*, 2014, **50**, 6574; S. E. R. Auty, O. C. J. Andrén, F. Y. Hern, M. Malkoch and S. P. Rannard, *Polym. Chem.*, 2015, **6**, 573; F. Y. Hern, S. E. R. Auty, O. C. J. Andrén, M. Malkoch and S. P. Rannard, *Polym. Chem.*, 2017, **8**, 1644.
13 A. B. Dwyer, P. Chambon, A. Town, T. He, A. Owen and S. P. Rannard, *Polym. Chem.*, 2014, **5**, 3608; A. B. Dwyer, P. Chambon, A. Town, F. L. Hatton, J. Ford and S. P. Rannard, *Polym. Chem.*, 2015, **6**, 7286.
14 T. He, D. J. Adams, M. F. Butler, A. I. Cooper and S. P. Rannard, *J. Am. Chem. Soc.*, 2009, **131**, 1495
15 J. Piella, N. G. Bastús and V. Puntes, *Chem. Mater.*, 2016, **28**, 1066.

Co-initiated hyperbranched-polydendron building blocks for the direct nanoprecipitation of dendron-directed patchy particles with heterogeneous surface functionality

Electronic Supporting Information

F. Y. Hern[a], A. Hill[a], A. Owen[b] and S. P. Rannard*[a]

[a]Department of Chemistry, University of Liverpool, Crown Street, Liverpool, L69 7ZD, UK.
[b]Department of Molecular and Clinical Pharmacology, University of Liverpool, Block H, Pembroke Place, Liverpool, L69 3GF, UK.
*E-mail: srannard@liverpool.ac.uk

Methods and Synthesis

Materials

All compounds were purchased from Sigma Aldrich unless otherwise stated and used without further purification. Potassium ethyl xanthogenate, 2-bromoacetic acid, pyridine, 4-dimethylaminopyridine (DMAP), 2,2-dimethoxypropane, N,N'-dicyclohexylcarbodiimide (DCC), benzyl acrylate and 2-(dimethylamino)ethyl acrylate (DMAEA) were purchased from Alfa Aesar and used without further purification. *Para*-toluene sulfonyl ethanol (*p*-TSe) was purchased from Fluorochem and used without further purification. Dichloromethane, hexane and ethyl acetate were HPLC grade and supplied by Fisher Scientific. Analytical TLC was performed on commercial Merck plates coated with silica gel. Flash chromatography was performed using a Grace Reveleris Flash System with Silica gel Flash Cartridges.

Analysis

Nuclear magnetic resonance (NMR): Spectra were recorded using a Bruker Avance 400 spectrometer, operating at 400 MHz for ^{1}H NMR and 100 MHz for ^{13}C NMR, in $CDCl_3$, CD_3OD or D_2O purchased from Goss Scientific. Chemical shifts (δ) are reported in parts per million (ppm) and TMS was used as an internal standard for both ^{1}H and ^{13}C spectra.

Mass Spectrometry (MS): Chemical ionisation (CI) mass spectra were obtained using an Agilent GC/Q-TOF 7200 instrument, using methane CI gas; whilst electrospray ionisation (ESI) mass spectra was obtained using a MicroMass LCT mass spectrometer using electron ionisation and direct infusion syringe pump sampling. All samples were diluted with methanol. Matrix-assisted laser desorption/ionisation - time of flight mass spectrometry (MALDI-TOF MS) sample solutions were prepared with a 2 mg/mL concentration in THF. Matrix solution was prepared at a concentration of 10 mg/mL in THF and 1 mg/mL Na counter ion solution was prepared. 5 μL of sample solution, 20 μL of matrix solution and 1.5 μL of counter ion was added to an Eppendorf sample tube and homogenised. Solution was deposited on a stainless steel sample plate and the solvent allowed to evaporate. Spectrum acquisitions were conducted on a Bruker UltraFlex MALDI-TOF MS with SCOUT-MTP Ion source (Bruker Daltonics, Bremen) equipped with a N_2-laser (337 nm), a gridless ion source and a reflector. All spectra were acquired using a reflector-positive method with an acceleration voltage of 25 kV and a reflector voltage of 26.3 kV. The detector mass range was set to exclude everything under 1000 Da in order to exclude high intensity peaks from the lower mass range. A total of 1000 shots were performed per sample and the laser intensity was set to the lowest possible value for acquisition of high resolution spectra. The instrument was calibrated using SpheriCal^{TM} calibrants purchased from Polymer Factory Sweden AB. The obtained spectra were analysed with FlexAnalysis Bruker Daltonics, Bremen, version 2.2.

Elemental microanalysis: Recorded on a Thermo FlashEA 1112 series CHNSO elemental analyser.

Size Exclusion Chromatography (SEC): Carried out using a Malvern Viscotek SEC Max equipped with a GPCmax VE2001 autosampler, two Viscotek T6000 columns (and a guard column), a refractive index detector VE3580 and a 270 Dual Detector (light scattering and viscometer) A mobile phase of THF containing 2%

triethylamine (v/v) at 35 °C, or DMF containing 0.01 M LiBr at 60 °C, was used as the eluent, with a flow rate of 1mL min^{-1}.

Dynamic light scattering (DLS): Measurements were carried out using a Malvern Zetasizer Nano ZS (4 mW He-Ne laser; wavelength 633 nm), at 25 °C using plastic disposable cuvettes for aqueous dispersions.

Transmission electron microscopy (TEM): Images were recorded using a Hitachi S-4800 FE-SEM at 20 kV. 10 µL of aqueous nanoparticle suspension was pipetted directly onto a Cu (holey carbon) 400 mesh 3 mm TEM grid (Agar Scientific) and blotted with filter paper.

Synthesis

Isopropylidene-2,2-bis(methoxy)propionic Acid **[Acet$_1$-G$_1$-COOH]**. 2,2-Bis(hydroxymethyl)-propionic acid (bis-MPA) (100 g, 0.746 mol, 1 equiv.), 2,2-dimethoxypropane (116.7 g, 137.24 mL, 1.12 mol, 1.5 equiv.), and *p*-toluenesulfonic acid monohydrate (7.09 g, 37.0 mmol, 0.05 equiv.) were added to 500 mL of acetone. The reaction mixture was stirred for 2 hours at ambient temperature (clear, colourless). After this time, the catalyst was neutralised by addition of 10 mL NH$_4$OH:EtOH (1:1 mixture), resulting in salt precipitation. The product was obtained by removal of acetone *in vacuo*, dissolving the crude solid in CH$_2$Cl$_2$ (750 mL), washing the organic layer twice with distilled water (2 x 300 mL), drying over MgSO$_4$ and evaporating to dryness. Yield: 100.86 g, white solid, (78%). ^{1}H NMR (400 MHz, CDCl$_3$): δ = 1.22 (s, 3H), 1.42 (s, 3H), 1.45 (s, 3H), 3.68 (d, *J* = 12.1 Hz, 2H), 4.20 (d, *J* = 12.1 Hz, 2H). ^{13}C NMR (100 MHz, CDCl$_3$): δ = 18.47, 21.92, 25.18, 41.86, 65.86, 98.43, 180.31. This compound was prepared by the procedure reported by Ihre *et al.*[1] Spectroscopic data agreed with those reported.

Isopropylidene-2,2-bis(methoxy)propionic Anhydride **[Acet$_2$-G$_1$-Anhy]**. [Acet$_1$-G$_1$-COOH] (88.94 g, 0.511 mol, 1 equiv.) and N,N'-Dicyclohexylcarbodiimide (DCC) (52.68 g, 0.255 mol, 0.50 equiv.) were added to 500 mL of CH$_2$Cl$_2$. The reaction mixture was stirred at ambient temperature for 48 hours. The precipitated N,N'-dicyclohexylurea (DCU) byproduct was removed by filtration and washed with a small volume of CH$_2$Cl$_2$. The crude product was purified by precipitating the filtrate into 2.5 L of cold hexane (cooled with dry ice bath) with vigorous stirring. Yield: 84.18 g, white viscous oil, (99%). ^{1}H NMR (400 MHz, CDCl$_3$): δ = 1.24 (s, 3H), 1.40 (s, 3H), 1.44 (s, 3H), 3.69 (d, *J* = 12.1 Hz, 4H), 4.21 (d, *J* = 12.1 Hz, 4H). ^{13}C NMR (100 MHz, CDCl$_3$): δ = 17.70, 21.73, 25.56, 43.59, 65.64, 98.42, 169.57. This compound was prepared from [Acet$_1$-G$_1$-COOH] according to the procedure reported by Malkoch *et al.*[2] Spectroscopic data agreed with those reported.

General esterification procedure for divergent dendron growth, [Acet$_1$-G$_1$-TSe]. [Acet$_1$-G$_1$-Anhy] (41.88 g, 127 mmol, 1.3 equiv.), *para*-toluene sulfonyl ethanol (*p*-TSe) (19.53 g, 98 mmol, 1 equiv.) and 4-dimethylaminopyridine (DMAP) (2.38 g, 20 mmol, 0.2 equiv.) were dissolved in anhydrous pyridine (40 mL, 5 equiv. per OH-group) and anhydrous CH$_2$Cl$_2$ (120 mL 1:3 ratio of pyridine:CH$_2$Cl$_2$ (v/v)) under a nitrogen atmosphere. The reaction was left to stir at ambient temperature for 16 hours, monitoring the reaction using TLC to confirm the loss of the starting alcohol. Following this, approximately 40 mL of distilled water was added and stirred vigorously at ambient temperature for an additional 2 hours to quench the excess anhydride. The product was isolated by diluting the mixture with CH$_2$Cl$_2$ (1 L) and washing with 1 M NaHSO$_4$ (3 x 400 mL), 1M

NaHCO$_3$ (3 x 400 mL), and brine (1 x 400 mL). The organic layer was dried over MgSO$_4$ and evaporated to dryness. Residual solvent was removed under high vacuum overnight. Purification by liquid chromatography on silica was not required for the isolation of [Acet$_1$-G$_1$-TSe]. Yield: 33.69 g, colourless viscous oil, (97%). ^{1}H NMR (400 MHz, CDCl$_3$): δ = 1.07 (s, 3H), 1.35 (s, 3H), 1.41 (s, 3H), 2.46 (s, 3H), 3.45 (t, 2H, J = 6.2 Hz), 3.56 (d, 2H, J = 11.9 Hz), 4.06 (d, 2H, J = 11.9 Hz), 4.45 (t, 2H, J = 6.2 Hz), 7.38 (d, 1H, J = 7.9 Hz), 7.81 (d, 1H, J = 7.9 Hz). ^{13}C NMR (100 MHz, CDCl$_3$): δ = 18.26, 21.62, 22.12, 25.09, 41.69, 55.06, 58.03, 65.75, 98.05, 128.17, 130.11, 136.14, 145.28, 173.72. Calcd: [MH]$^+$ (C$_{17}$H$_{25}$O$_6$S) = 357.13 Da. Found: CI-MS: [MH]$^+$ = 357.14 Da. Anal. Calcd for C$_{17}$H$_{24}$O$_6$S: C, 57.28; H, 6.79; S, 9.00. Found: C, 57.30; H, 6.81; S, 8.89.

General deprotection procedure for removal of acetonide protecting groups, [(OH)$_2$-G$_1$-TSe]. DOWEX 50W-X2 (approx. 6 g) was added to a solution of [Acet$_1$-G$_1$-TSe] (34.73 g, 97 mmol, 1 equiv.) in methanol (350 mL) and allowed to stir at 50 °C for 3 hours. The deprotection was monitored by TLC until total disappearance of the starting material resulted. Once complete, the resin was filtered off and the solution evaporated to dryness. Residual solvent was removed under high vacuum overnight. Yield: 30.49 g, white crystals, (99%). ^{1}H NMR (400 MHz, CD$_3$OD): δ = 1.05 (s, 3H), 2.47 (s, 3H), 3.15 (s, br, 1H), 3.44 (t, 2H, J = 5.8 Hz), 3.73 (d, 2H, J = 11.6 Hz), 3.85 (d, 2H, J = 11.6 Hz), 4.53 (t, 2H, J = 5.8 Hz), 7.39 (d, 2H, J = 8.0 Hz), 7.80 (d, 2H, J = 8.0 Hz). ^{13}C NMR (100 MHz, CD$_3$OD): δ = 17.06, 21.74, 49.65, 55.14, 57.42, 67.96, 128.07, 130.22, 135.55, 145.57, 175.22. Calcd: [M+Na]$^+$ (C$_{14}$H$_{20}$NaO$_6$S) = 339.10 Da. Found: ESI-MS: [M+Na]$^+$ = 339.10 Da. Anal. Calcd for C$_{14}$H$_{20}$O$_6$S: C, 53.15; H, 6.37; S, 10.14. Found: C, 53.29; H, 6.44; S, 10.01.

[Acet$_2$-G$_2$-TSe]. [(OH)$_2$-G$_1$-TSe] (14.73 g, 46.56 mmol, 1 equiv.), DMAP (2.56 g, 20.95 mmol, 0.45 equiv.), [Acet$_2$-G$_1$-Anhy] (46.15 g, 139.68 mmol, 3 equiv.), 38 mL pyridine and 114 mL CH$_2$Cl$_2$ were reacted according to the general esterification procedure, resulting in a viscous colourless oil that was purified by liquid chromatography on silica, eluted from EtOAc:hexane (10:90) increasing the polarity to EtOAc:hexane (50:50). Yield: 26.35 g, colourless viscous oil, (90%). ^{1}H NMR (400 MHz, CDCl$_3$): δ = 1.11 (s, 6H), 1.17 (s, 3H), 1.34 (s, 6H), 1.41 (s, 6H), 2.46 (s, 3H), 3.45 (t, 2H, J = 6.2 Hz), 3.61 (d, 4H, J = 11.9 Hz), 4.13 (d, 4H, J = 11.9 Hz), 4.18 (d, 2H, J = 11.1 Hz), 4.21 (d, 2H, J = 11.1 Hz), 4.45 (t, 2H, J = 6.2 Hz), 7.38 (d, 2H, J = 8.1 Hz), 7.80 (d, 2H, J = 8.1 Hz).^{13}C NMR (100 MHz, CDCl$_3$): δ = 17.37, 18.42, 21.65, 25.68, 42.09, 46.64, 54.83, 58.32, 65.06, 65.98, 65.98, 98.09, 128.05, 130.20, 136.24, 145.24, 171.98, 173.46. Calcd: [M+Na]$^+$ (C$_{30}$H$_{44}$NaO$_{12}$S) = 651.73 Da. Found: ESI-MS: [M+Na]$^+$ = 651.20 Da. Anal. Calcd for C$_{30}$H$_{44}$O$_{12}$S: C, 57.31; H, 7.05; S, 5.10. Found: C, 58.10; H, 7.16; S, 4.72.

[(OH)$_4$-G$_2$-TSe]. DOWEX 50W-X2 (approx. 5 g) and [Acet$_2$-G$_2$-TSe] (25.26 g, 40.18 mmol, 1 equiv) dissolved in methanol (250 mL) was reacted according to the general deprotection procedure. Yield: 20.72 g, white crystals, (99%). ^{1}H NMR (400 MHz, CD$_3$OD): δ = 1.13 (s, 9H), 2.46 (s, 3H), 3.58 (s, 2H), 3.66 (d, 4H, J = 10.8 Hz), 3.69 (d, 4H, J = 10.8 Hz), 4.09 (d, 2H, J = 11.2 Hz), 4.14 (d, 2H, J = 11.2 Hz), 4.43 (t, 2H, J = 5.6 Hz), 7.47 (d, 2H, J = 8.2 Hz), 7.82 (d, 2H, J = 8.2 Hz). ^{13}C NMR (100 MHz, CD$_3$OD): δ = 17.32, 18.46, 21.54, 25.56, 42.05, 46.66, 54.90, 58.35, 65.06, 66.00, 98.04, 128.15, 130.07, 136.20, 145.22, 172.06, 173.40. Calcd: [M+Na]$^+$ (C$_{24}$H$_{36}$NaO$_{12}$S) = 571.18 Da. Found: ESI-MS: [M+Na]$^+$ = 571.20 Da. Anal. Calcd for C$_{24}$H$_{36}$O$_{12}$S: C, 52.54; H, 6.61; S, 5.84. Found: C, 52.49; H, 6.56; S, 5.31.

[Acet$_4$-G$_3$-TSe]. **[**(OH)$_4$-G$_2$-TSe] (5.89 g, 11 mmol, 1 equiv.), DMAP (0.81 g, 7 mmol, 0.62 equiv.), [Acet$_2$-G$_1$-Anhy] (21.27 g, 64 mmol, 6 equiv.), 53 mL pyridine and 160 mL CH$_2$Cl$_2$ were reacted according to the general esterification procedure, resulting in a viscous colourless oil that was purified by liquid chromatography on silica, eluted from EtOAc:hexane (20:80) increasing the polarity to EtOAc:hexane (60:40). Yield: 12.46 g, colourless viscous oil, (99%). ^{1}H NMR (400 MHz, CDCl$_3$): δ = 1.14 (s, 12H), 1.18 (s, 3H), 1.27 (s, 6H), 1.35 (s, 12H), 1.41 (s, 12H), 2.46 (s, 3H), 3.46 (t, 2H, J = 6.0 Hz), 3.6 (d, 8H, J = 12.1 Hz) 4.08-4.22 (m, 12H), 4.25-4.35 (m, 8H), 4.48 (t, 2H, J = 6.0 Hz), 7.39 (d, 2H), 7.82 (d, 2H).^{13}C NMR (100 MHz, CDCl$_3$): δ = 17.25, 17.68, 18.44, 21.67, 22.01, 25.20, 42.05, 46.63, 46.93, 54.74, 58.32, 64.95, 65.76, 65.93, 65.98, 98.07, 128.15, 130.13, 136.23, 145.11, 171.67, 171.88, 173.47. Calcd: [M+Na]$^+$ (C$_{56}$H$_{84}$NaO$_{24}$S) = 1195.50 Da. Found: ESI-MS: [M+Na]$^+$ = 1195.50 Da. Anal. Calcd for C$_{56}$H$_{84}$O$_{24}$S: C, 57.32; H, 7.22; S, 2.73. Found: C, 57.33; H, 7.18; S, 2.35.

[(OH)$_8$-G$_3$-TSe]. DOWEX 50W-X2 (approx. 4 g) and [Acet$_4$-G$_3$-TSe] (22.66 g, 19 mmol, 1 equiv) dissolved in methanol (300 mL) was reacted according to the general deprotection procedure. Yield: 19.44 g, white crystals, (99%). ^{1}H NMR (400 MHz, CD$_3$OD): δ = 1.17 (s, 15H), 1.30 (s, 6H), 2.49 (s, 3H), 3.56- 3.73 (m, 18H), 4.14-4.38 (m, 12H), 4.49 (t, 2H, J = 5.5 Hz), 7.51 (d, 2H), 7.87 (d, 2H). ^{13}C NMR (100 MHz, CD$_3$OD): δ = 17.40, 17.71, 18.35, 21.61, 47.74, 47.88, 51.91, 55.75, 59.77, 65.91, 66.15, 67.06, 129.38, 131.30, 138.01, 146.83, 173.33, 173.70, 175.97. Calcd: [M+Na]$^+$ (C$_{44}$H$_{68}$NaO$_{24}$S) = 1035.37 Da. Found: ESI-MS: [M+Na]$^+$ = 1035.40 Da. Anal. Calcd for C$_{44}$H$_{68}$O$_{24}$S: C, 52.17; H, 6.77; S, 3.17. Found: C, 51.97; H, 6.65; S, 3.15.

2-((Ethoxycarbonothioyl)thio)acetic acid **[Xan-COOH]**. Potassium ethyl xanthogenate (53.06 g, 331 mmol) was stirred in acetone (400 mL). A solution of 2-bromoacetic acid (38.35 g, 276 mmol) in acetone (100 mL) was added dropwise over 20 minutes. The reaction was left to stir overnight at ambient temperature. The precipitated potassium bromide by-product was filtered off and washed with a small volume of acetone. The solvent was removed under vacuum. The residue was then diluted in CH$_2$Cl$_2$ (300 mL) and washed with brine (3 x 100 mL). The organic phase was dried over MgSO$_4$ and evaporated to give [Xan-COOH] as a pale yellow solid. Yield: 36.35g (73%) ^{1}H NMR (400 MHz, CDCl$_3$): δ = 1.43 (t, 3H, J = 7.2 Hz), 3.96 (s, 2H), 4.66 (q, 2H, J = 7.2 Hz), 9.12 (s, 1H, br). ^{13}C NMR (100 MHz, CDCl$_3$): δ 13.79, 37.56, 70.99, 174.13, 212.0.

2-((Ethoxycarbonothioyl)thio)acetic anhydride **[Xan-Anhy]**. [Xan-COOH] (27.53 g, 152 mmol, 1 equiv.) was dissolved in 100 mL CH$_2$Cl$_2$. A solution N,N′-Dicyclohexylcarbodiimide (DCC) (20.76 g, 101 mmol, 0.5 equiv.) in CH$_2$Cl$_2$ was slowly added to the mixture, and the reaction allowed to stir at ambient temperature overnight. The reaction was monitored by ^{13}C NMR. Determination of reaction completion resulted by the appearance of the anhydride carbonyl carbon at 163 ppm and the disappearance of the acid carbonyl carbon at 174 ppm. The dicyclohexylurea (DCU) by-product was removed by filtration, washed with a small volume of CH$_2$Cl$_2$ and the solvent evaporated under vacuum. Yield: 26.00 g, yellow solid, (99%). ^{1}H NMR (400 MHz, CDCl$_3$): δ = 1.44 (t, 6H, J = 7.1 Hz) 4.07 (s, 4H), 4.67 (q, 4H, J = 7.1 Hz). ^{13}C NMR (100 MHz, CDCl$_3$): δ = 13.64, 38.51, 71.28, 163.04, 211.44.

General procedure for functionalisation with Xanthate surface groups using anhydride chemistry, [Xan$_8$-G$_3$-TSe]. This compound was prepared by the procedure reported by Auty *et al.*[3] [(OH)$_8$-G$_3$-TSe] (7.24 g, 7 mmol, 1 equiv.) and DMAP (1.40 g, 11 mmol, 1.6 equiv.) were dissolved in anhydrous pyridine (40 mL). After cooling the mixture in an ice bath, [Xan-Anhy] (25.41 g, 74 mmol, 10.4 equiv.) in anhydrous CH$_2$Cl$_2$ (80 mL) was added slowly under a nitrogen atmosphere. After stirring at ambient temperature for 16 hours, approximately 15 mL of distilled water was added and stirred vigorously at ambient temperature for an additional 2 hours to quench the excess anhydride. The product was isolated by diluting the mixture with CH$_2$Cl$_2$ (350 mL) and washing with 1 M NaHSO$_4$ (3 x 1200 mL), 1M NaHCO$_3$ (3 x 200 mL), and brine (1 x 200 mL). The organic layer was dried over MgSO$_4$ and evaporated to dryness. Purification by liquid chromatography on silica, eluted from EtOAc:hexane (15:85) increasing the polarity to EtOAc:hexane (50:50). Residual solvent was removed under high vacuum overnight. Yield: 10.10 g, orange viscous oil, (61%). ^{1}H NMR (400 MHz, CDCl$_3$): δ = 1.20-1.30 (m, 21H), 1.42 (t, 24H, *J* = 7.2 Hz), 2.47 (s, 3H), 3.47 (t, 2H, *J* = 5.8 Hz), 3.94 (s, 16H), 4.16-4.36 (m, 28H), 4.49 (t, 2H, *J* = 5.8 Hz), 4.64 (q, 16H, *J* = 7.2 Hz) 7.40 (d, 2H), 7.81 (d, 2H). ^{13}C NMR (100 MHz, CDCl$_3$): δ = 13.67, 17.28, 17.63, 17.89, 21.73, 37.64, 46.27, 46.51, 46.75, 54.71, 58.35, 65.44, 66.23, 70.82, 128.15, 130.26, 136.39, 145.22, 167.46, 171.48, 171.63, 171.68, 212.71. Calcd: [M+Na]$^+$ (C$_{84}$H$_{116}$NaO$_{40}$S$_{17}$) = 2331.22 Da. Found: MALDI-TOF MS: [M+Na]$^+$ = 2331.42 Da. Anal. Calcd for C$_{84}$H$_{116}$O$_{40}$S$_{17}$: C, 43.66; H, 5.06; S, 23.59. Found: C, 44.01; H, 5.04; S, 23.86.

General procedure for deprotection of *para*-toluene sulfonyl ester (TSe) - 1,8- diazabicyclo[5.4.0]undec-7-ene (DBU) (1.3 equiv.) added to xanthate functional dendron dissolved in anhydrous CH$_2$Cl$_2$. The reaction was stirred under a nitrogen atmosphere for 16 hours and monitored by using TLC (40:60 ethyl acetate:hexane). The product was isolated by diluting the mixture with CH$_2$Cl$_2$ (100 mL) and washing with 1 M NaHSO$_4$ (2 x 100 mL). The organic layer was dried over MgSO$_4$ and evaporated to dryness. The product was then precipitated three times into hexane:ethyl acetate (9:1). Any residual solvent was removed under high vacuum to yield a viscous oil.

[Xan$_8$-G$_3$-COOH]. The removal of the *para*-toluene sulfonyl (*p*-TSe) protecting group was carried out as described above with [Xan$_8$-G$_3$-TSe] (9.07 g, 3.93 mmol, 1.0 equiv), and DBU (0.76 mL, 5.10 mmol, 1.3 equiv). Yield: 7.97 g, orange viscous oil (95%). ^{1}H NMR (400 MHz, CDCl$_3$): δ = 1.26 (s, 12H), 1.29 (s, 6H), 1.35 (s, 3H), 1.42 (t, *J* = 7.1 Hz, 24H), 3.95 (s, 16H), 4.21-4.36 (m, 28H), 4.64 (q, *J* = 7.1 Hz, 16H). ^{13}C NMR (100 MHz, CDCl$_3$): δ = 13.70, 17.98, 37.70, 46.41, 66.30, 70.91, 167.70, 171.65, 172.95, 212.57. Calcd: [M+Na]$^+$ (C$_{75}$H$_{106}$NaO$_{38}$S$_{16}$) m/z = 2149.19. Found MALDI-TOF: [M+Na]$^+$ m/z = 2151.7. Anal. Calcd for C$_{75}$H$_{106}$O$_{38}$S$_{16}$: C, 42.32; H, 5.02; S, 28.56. Found: C, 43.15; H, 5.09; S, 23.79.

2-Hydroxyethyl-2-bromoisobutyrate, **[HEBiB]**. Ethylene glycol (272 mL, 4.85 mol, 50 equiv.) and triethylamine (TEA) (28 mL, 0.20 mol, 2 equiv.) were dissolved in anhydrous THF (100 mL). α-Bromoisobutyryl bromide (12 mL, 97.1 mmol, 1 equiv.) was added dropwise over 30 minutes whilst cooling with an ice bath. The reaction was left to stir at ambient temperature under a nitrogen atmosphere for 16 hours. The product was isolated by pouring the crude mixture into distilled water (800 mL) and extracting the aqueous phase with CH$_2$Cl$_2$ (6 x 100 mL). The combined organic layers were washed with 1 M HCl (pH 4) (2 x 300mL),

dried over $MgSO_4$ and evaporated to dryness. Residual solvent was removed under high vacuum overnight. Yield: 15.64 g, pale yellow oil, (76%) ^{1}H NMR (400 MHz, $CDCl_3$): δ = 1.96 (s, 6H), 3.88 (t, J = 4.7 Hz, 2H), 4.32 (t, J = 4.7 Hz, 2H). ^{13}C NMR (100 MHz, $CDCl_3$): δ = 30.70, 55.86, 60.82, 67.47, 171.94. Calcd: $[M+NH_4]^+$ ($C_6H_{15}BrNO_3$) m/z = 228.02. Found: CI MS: $[M+NH_4]^+$ m/z = 228.02. Anal. Calcd for $C_6H_{11}BrO_3$: C, 34.14; H, 5.25. Found: C, 34.63; H, 5.30. This compound was prepared by Jakubowski et al.[4] The above spectroscopic data agreed with that reported.

4-(Dimethylamino)pyridinium p-toluenesulfonate **[DPTS]** – p-toluenesulfonic acid monohydrate (7.80 g, 41 mmol, 1 equiv) was dried by azeotropic distillation with 50 mL anhydrous toluene using a dean-stark head (approximately 4 hours). [Note: the solution turned dusty pink during the loss of water]. Following this, the mixture was cooled to 60 °C and 4-dimethylaminopyridine (DMAP) (5 g, 41 mmol, 1 equiv.) in 30 mL of anhydrous toluene at 60 °C added slowly. An off-white precipitate immediately formed upon addition, and the solution was left to stir at 60 °C for 1 hour. The mixture was then cooled and filtered to yield DPTS. The product was recrystallised once from 1,2-dichloroethane to yield white crystals. Yield: 11.83 g (98%). ^{1}H NMR (400 MHz, $CDCl_3$): δ = 2.34 (s, 3H), 3.17 (s, 6H), 6.76 (d, J = 7.7 Hz, 2H), 7.16 (d, J = 8.2 Hz, 2H), 7.81 (d, J = 8.2 Hz, 2H), 8.16 (d, J = 7.7 Hz, 2H). ^{13}C NMR (100 MHz, $CDCl_3$): δ = 21.34, 40.15, 106.86, 126.00, 128.72, 139.49, 142.76, 157.26. Anal. Calcd for $C_{14}H_{18}N_2O_3S$: C, 57.12; H, 6.16; N, 9.52; S, 10.89. Found: C, 57.30; H, 6.12; N, 9.51; S, 10.84. This compound was prepared by the procedure reported by Moore and Stupp. The above spectroscopic data agreed with that reported.[5]

General procedure for focal point modification to α-bromoisobutyrate moiety, [Xan$_1$-G$_0$-BiB]. **[Xan-COOH]** (2.42 g, 13 mmol, 1 equiv.), **[HEBiB]** (2.83 g, 13 mmol, 1 equiv.), and DPTS (4.33 g, 15 mmol, 1.1 equiv.) were dissolved in CH_2Cl_2 (anhydrous, 35 mL) under a nitrogen atmosphere. DCC (3.04 g, 15 mmol, 1.1 equiv.) in CH_2Cl_2 (anhydrous, 15 mL) was added and the reaction left to stir at ambient temperature for 16 hours. The precipitated DCU by-product was removed by filtration and the product isolated by diluting the mixture with CH_2Cl_2 (100 mL), washing with distilled water (2 x 100 mL) and brine (1 x 100 mL). The organic layer was dried over $MgSO_4$ and evaporated to dryness. The residue was purified by liquid chromatography on silica, eluting from ethyl acetate:hexane (10:90), gradually increasing the polarity to ethyl acetate:hexane (30:70). Residual solvent was removed under high vacuum overnight. Yield: 3.74 g, yellow oil, (75%). ^{1}H NMR (400 MHz, $CDCl_3$): δ = 1.42 (t, J = 7.1 Hz, 3H), 1.94 (s, 6H), 3.96 (s, 2H), 4.41 (s, 4H), 4.65 (q, J = 7.1 Hz, 2H). ^{13}C NMR (100 MHz, $CDCl_3$): δ = 13.48, 30.36, 37.44, 55.09, 62.95, 70.43, 167.46, 171.10, 212.14. Calcd: $[M+Na]^+$ ($C_{11}H_{17}BrNaO_5S_2$) m/z = 394.97. Found: ESI-MS: $[M+Na]^+$ m/z = 395.0 Anal. Calcd for $C_{11}H_{17}BrO_5S_2$: C, 35.39; H, 4.59; S, 17.18. Found: C, 35.76; H, 4.57; S, 16.76.

[Xan$_8$-G$_3$-BiB]. **[Xan$_8$-G$_3$-COOH]** (3.98 g, 1.87 mmol, 1 equiv.), **[HEBiB]** (0.40 g, 1.87 mmol, 1 equiv.), DPTS (0.61 g, 2.06 mmol, 1.1 equiv.), DCC (0.42 g, 2.06 mmol, 1.1 equiv.) in anhydrous CH_2Cl_2 (40 mL) were reacted according to the general procedure for focal point modification resulting in a viscous orange oil that was purified by liquid chromatography on silica, eluting from ethyl acetate:hexane (15:85), gradually increasing the polarity to ethyl acetate:hexane (50:50). Yield: 2.47 g, orange viscous oil, (57%). ^{1}H NMR (400 MHz, $CDCl_3$): δ = 1.26 (s, 12H), 1.28 (s, 6H), 1.32 (s, 3H), 1.42 (t, J = 7.1 Hz, 24H), 1.94 (s, 6H), 3.95 (s, 16H), 4.21-4.38 (m,

28H), 4.21 (s, 4H), 4.64 (q, J = 7.1 Hz, 16H). ^{13}C NMR (100 MHz, CDCl$_3$): δ = 13.67, 17.89, 30.74, 37.64, 46.27, 55.48, 60.85, 66.21, 70.82, 167.46, 171.67, 212.71. Calcd: [M+Na]$^+$ (C$_{81}$H$_{115}$BrNaO$_{40}$S$_{16}$) m/z = 2341.17. Found: MALDI-TOF: [M+Na]$^+$ m/z = 2341.4. Anal. Calcd for C$_{81}$H$_{115}$BrO$_{40}$S$_{16}$: C, 41.91; H, 4.99; S, 22.09. Found: C, 43.15; H, 5.14; S, 21.85.

Linear ATRP of _n_-butyl methacrylate (_n_-BuMA) in methanol with [Xan$_1$-G$_0$-BiB] and [Xan$_8$-G$_3$-BiB], targeting DP$_n$ = 100 monomer units; G$_0$-p(_n_-BuMA)$_{100}$, G$_3$-p(_n_-BuMA)$_{100}$. In a typical synthesis, targeting DP$_n$ = 100 monomer units for the primary chains, [Xan$_1$-G$_0$-BiB] (46 mg, 0.0702 mmol, 1 equiv.), _n_-BuMA (1 g, 7.03 mmol, 100 equiv.) and 2,2'-bipyridyl (bpy) (22 mg, 0.141 mmol, 2 equiv.) were placed into a 5 mL round-bottomed flask. Methanol was added (50 wt% based on _n_-BuMA; 2g, 2.6 mL) and the solution stirred and deoxygenated using a nitrogen purge for 30 minutes. Cu(I)Cl (7 mg, 0.0702 mmol, 1 equiv) was added to the flask, whilst maintaining a positive flow of nitrogen, and the solution left to polymerise at 60 °C. The reaction was terminated when conversion reached >95%, indicated by ^{1}H NMR after 21 hours, by exposure to oxygen and addition of THF. The solution was passed through a neutral alumina column to remove the catalytic system, and precipitated twice into cold petroleum ether (40-60 °C). After drying the precipitated sample overnight under high vacuum, the polymer was obtained as a white solid. This compound was prepared by the procedure reported by Hern _et al._[6]

[PEG$_{45}$-BiB]. Monomethoxy poly(ethylene glycol) (M$_w$ ≈ 2000 g mol^{-1}) (10.25 g, 5.13 mmol, 1 equiv.) was dissolved in THF (anhydrous, 100 mL) at 40 °C, and degassed with dry N$_2$ for 20 minutes. DMAP (6.26 mg, 0.0512 mmol, 0.01 equiv.) and TEA (1.57 mL, 11 mmol, 2.2 equiv.) were added and the reaction cooled to 0 °C in an ice bath. α-Bromoisobutyryl bromide (1.27 mL, 10 mmol, 2 equiv.) was added dropwise over 20 minutes and a white precipitate immediately formed (Et$_3$NH$^+$Br$^-$ salt). After 24 hours, the precipitate was removed by filtration, THF removed and the crude material precipitated twice from acetone into petroleum ether (30-40 °C). ^{1}H NMR (400 MHz, D$_2$O): δ = 4.30-4.35 (m, 2H), 3.59-3.80 (m, 186H), 3.35 (s, 3H), 1.93 (s, 6H).

p(PEG$_{45}$-_b_-_n_-BuMA$_{100}$). In a kinetics study, targeting DP$_n$ = 100 monomer units for the primary chains, [PEG$_{45}$-BiB] (0.302 g, 0.141 mmol, 1 equiv.), _n_-BuMA (2 g, 14 mmol, 100 equiv.) and bpy (44 mg, 0.282 mmol, 2 equiv.) were placed into a 10 mL round-bottomed flask. Methanol was added (50 wt% based on _n_-BuMA; 2g, 2.6 mL) and the solution stirred and deoxygenated using a nitrogen purge for 30 minutes. Cu(I)Cl (14 mg, 0.141 mmol, 1 equiv) was added to the flask, whilst maintaining a positive flow of nitrogen, and the solution left to polymerise at 60 °C. To determine the kinetics of the reaction, samples (~0.1 mL) were taken at regular intervals and analysed by ^{1}H NMR and SEC. The reaction was terminated when conversion reached >94%, indicated by ^{1}H NMR after 28 hours, by exposure to oxygen and addition of THF. The solution was passed through a neutral alumina column to remove the catalytic system, and precipitated twice into cold petroleum ether (40-60 °C). After drying the precipitated sample overnight under high vacuum, the polymer was obtained as a white solid.

General procedure for the co-initiated branched copolymerisation of *n*-BuMA and EGDMA with [Xan$_1$-G$_0$-BiB] and [PEG$_{45}$-BiB]; [(G$_0$)$_{0.01}$-(PEG$_{45}$)$_{0.99}$]-p(*n*-BuMA$_{100}$-*co*-EGDMA$_{0.8}$), [(G$_0$)$_{0.075}$-(PEG$_{45}$)$_{0.925}$]-p(*n*-BuMA$_{100}$-*co*-EGDMA$_{0.8}$), [(G$_0$)$_{0.1}$-(PEG$_{45}$)$_{0.9}$]-p(*n*-BuMA$_{100}$-*co*-EGDMA$_{0.8}$). The co-initiated copolymerisation of *n*-BuMA and bifunctional monomer EGDMA was carried out with varying molar equivalents of [PEG$_{45}$-BiB] and [Xan$_1$-G$_0$-BiB] (99:1, 92.5:7.5, 90:10). In a typical synthesis, targeting DP$_n$ = 100 monomer units for the primary chains, [PEG$_{45}$-BiB], [Xan$_1$-G$_0$-BiB], *n*-BuMA (5 g, 35 mmol, 100 equiv.), bpy (110 mg, 0.703 mmol, 2 equiv.) and EGDMA (56 mg, 0.280 mmol, 0.8 equiv.) were placed into a 20 mL round-bottomed flask. Methanol was added (50 wt% based on *n*-BuMA, 5g, 7.5 mL) and the solution stirred and deoxygenated using a nitrogen purge for 30 minutes. Cu(I)Cl (35 mg, 0.352 mmol, 1 equiv) was added to the flask, whilst maintaining a positive flow of nitrogen, and the solution was left to polymerise at 60 °C. The reaction was terminated when conversion reached >98%, indicated by ^{1}H NMR after 70 hours, by exposure to oxygen and addition of THF. The solution was passed through a neutral alumina column to remove the catalytic system, and precipitated twice into cold petroleum ether (40-60 °C). After drying the precipitated sample overnight under high vacuum, the polymer was obtained as a white solid.

General procedure for the co-initiated branched copolymerisation of *n*-BuMA and EGDMA with [Xan$_8$-G$_3$-BiB] and [PEG$_{45}$-BiB]; [(G$_3$)$_{0.01}$-(PEG$_{45}$)$_{0.99}$]-p(*n*-BuMA$_{100}$-*co*-EGDMA$_{0.8}$), [(G$_3$)$_{0.014}$-(PEG$_{45}$)$_{0.986}$]-p(*n*-BuMA$_{100}$-*co*-EGDMA$_{0.8}$), [(G$_3$)$_{0.05}$-(PEG$_{45}$)$_{0.95}$]-p(*n*-BuMA$_{100}$-*co*-EGDMA$_{0.8}$). The co-initiated copolymerisation of *n*-BuMA and bifunctional monomer EGDMA was carried out with varying molar equivalents of [PEG$_{45}$-BiB] and [Xan$_8$-G$_3$-BiB] (99:1, 98.6:1.4, 95:5). In a typical synthesis, targeting DP$_n$ = 100 monomer units for the primary chains, [PEG$_{45}$-BiB], [Xan$_8$-G$_3$-BiB], *n*-BuMA (5 g, 35 mmol, 100 equiv.), bpy (110 mg, 0.703 mmol, 2 equiv.) and EGDMA (56 mg, 0.280 mmol, 0.8 equiv.) were placed into a 20 mL round-bottomed flask. Methanol was added (50 wt% based on *n*-BuMA, 5g, 7.5 mL) and the solution stirred and deoxygenated using a nitrogen purge for 30 minutes. Cu(I)Cl (35 mg, 0.352 mmol, 1 equiv.) was added to the flask, whilst maintaining a positive flow of nitrogen, and the solution was left to polymerise at 60 °C. The reaction was terminated when conversion reached >98%, indicated by ^{1}H NMR after 72 hours, by exposure to oxygen and addition of THF. The solution was passed through a neutral alumina column to remove the catalytic system, and precipitated twice into cold petroleum ether (40-60 °C). After drying the precipitated sample overnight under high vacuum, the polymer was obtained as a white solid.

4 nm GNP synthesis. Prepared by the Inverse Turkevich procedure reported by Piella *et al.*[7] Sodium citrate (2.2 mM, 150 mL), tannic acid (2.5 mM, 0.1 mL) and K$_2$CO$_3$ (150 mM, 1 mL) were stirred at 70°C, followed by addition of HAuCl$_4$ (25 mM, 1 mL), then allowed to react for 20 minutes with vigorous stirring. The solution was then cooled to ambient temperature and stored in polyethylene centrifuge tubes.

General procedure for the deprotection of peripheral xanthate groups of co-initiated HPDs, and subsequent nanoprecipitation and coordination of 4 nm GNPs. Peripheral xanthate groups of each polymer (200 mg, 1 equiv.) were deprotected with excess *n*-butylamine (10 equiv.) in THF (anhydrous, 2 mL) for 1.5 hours. The deprotected polymer was precipitated twice into hexane and dried under vacuum. The deprotected polymer was dissolved in acetone at an initial concentration of 5 mg/mL. The dissolved polymer was rapidly

added to water with stirring at ambient temperature. The solvent was allowed to evaporate overnight to give nanoprecipitates with a final concentration of 1 mg/mL of polymer in water. A 1:9 ratio of polymer nanoprecipitates:4 nm GNPs was mixed and stirred for 24 hours, before imaging by TEM.

TEM preparation. TEM grids (3 mm, 400 mesh Cu(holey carbon)) were prepared by pipetting 10 µL of the polymer/GNP samples directly onto the carbon coated side of the grid, and immediately wicking away excess water with filter paper. The grids were allowed to dry for 24 hours before imaging.

1. H. Ihre, A. Hult, J. M. J. Fréchet en I. Gitsov, *Macromolecules*, 1998, **31**, 4061–4068.
2. M. Malkoch, E. Malmström en A. Hult, *Macromolecules*, 2002, **35**, 8307–8314.
3. S. E. R. Auty, O. C. J. Andrén, F. Y. Hern, M. Malkoch en S. P. Rannard, *Polym. Chem.*, 2014, **6**, 573–582.
4. W. Jakubowski, J. F. Lutz, S. Slomkowski en K. Matyjaszewski, *J. Polym. Sci. Part A Polym. Chem.*, 2005, **43**, 1498–1510.
5. J. S. Moore en S. I. Stupp, *Macromolecules*, 1990, **23**, 65–70.
6. F. Y. Hern, S. E. R. Auty, O. C. J. Andren, M. Malkoch en S. P. Rannard, *Polym. Chem.*, 2017, **8**, 1644–1653.
7. J. Piella, N. G. Bastús en V. Puntes, *Chem. Mater.*, 2016, **28**, 1066–1075.

Figure S1. ^{1}H NMR (400 MHz, CDCl$_3$) of **[Acet$_1$-G$_1$-COOH]**

Figure S2. ^{13}C NMR (100 MHz, CDCl$_3$) of **[Acet$_1$-G$_1$-COOH]**

Figure S3. ^{1}H NMR (400 MHz, CDCl$_3$) of **[Acet$_1$-G$_1$-Anhy]**
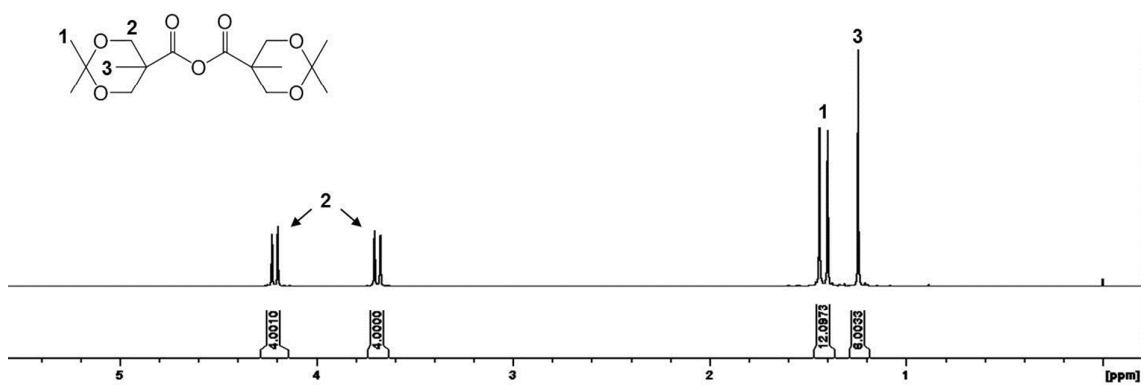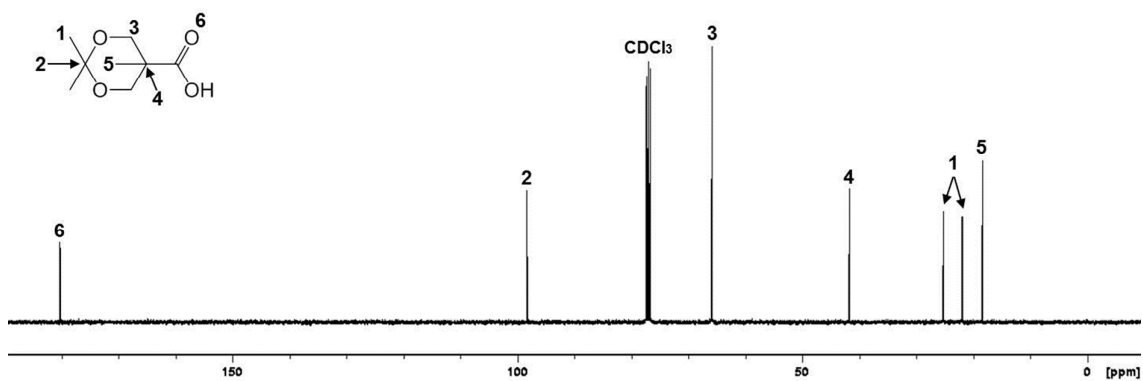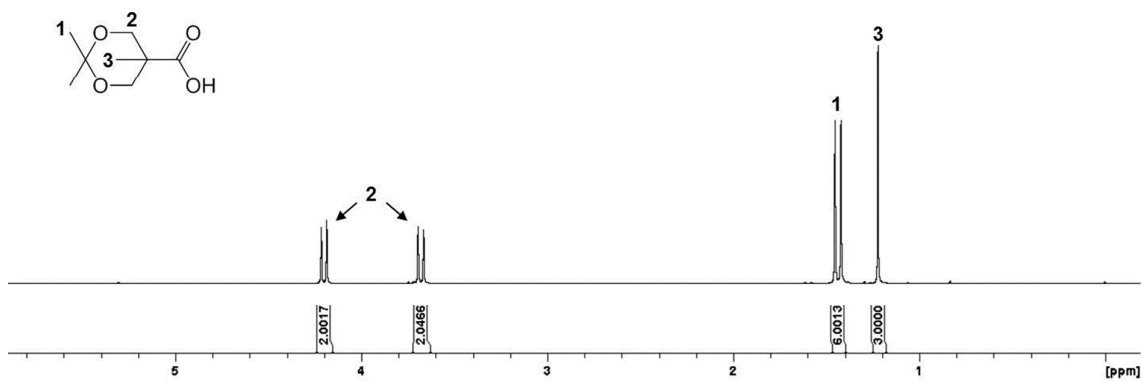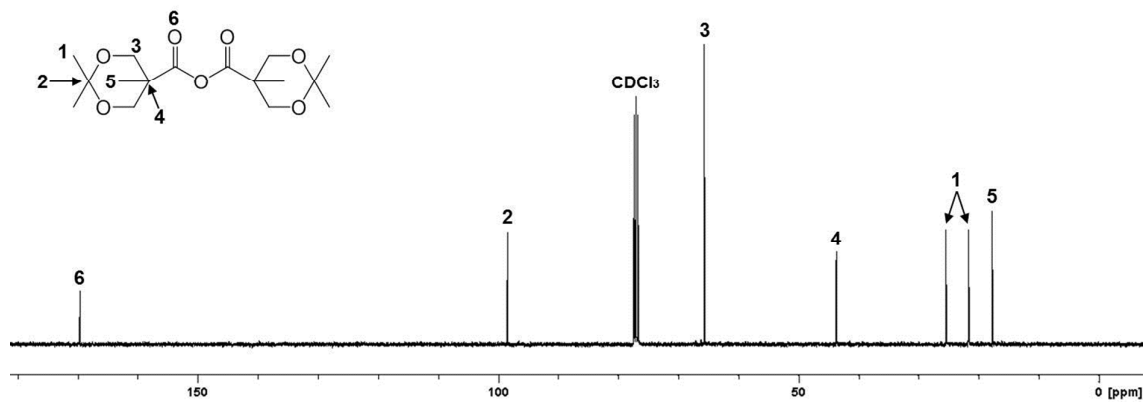
Figure S4. ^{13}C NMR (100 MHz, CDCl$_3$) of **[Acet$_1$-G$_1$-Anhy]**
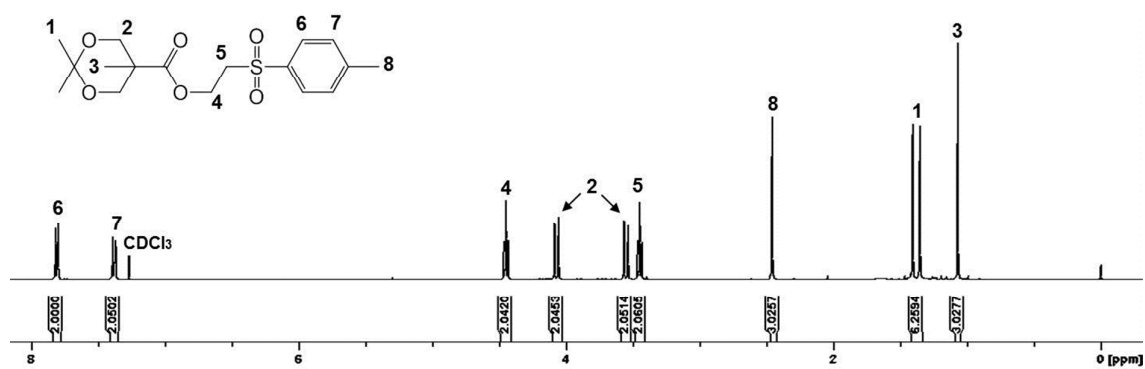
Figure S5. ^{1}H NMR (400 MHz, CDCl$_3$) of **[Acet$_1$-G$_1$-TSe]**
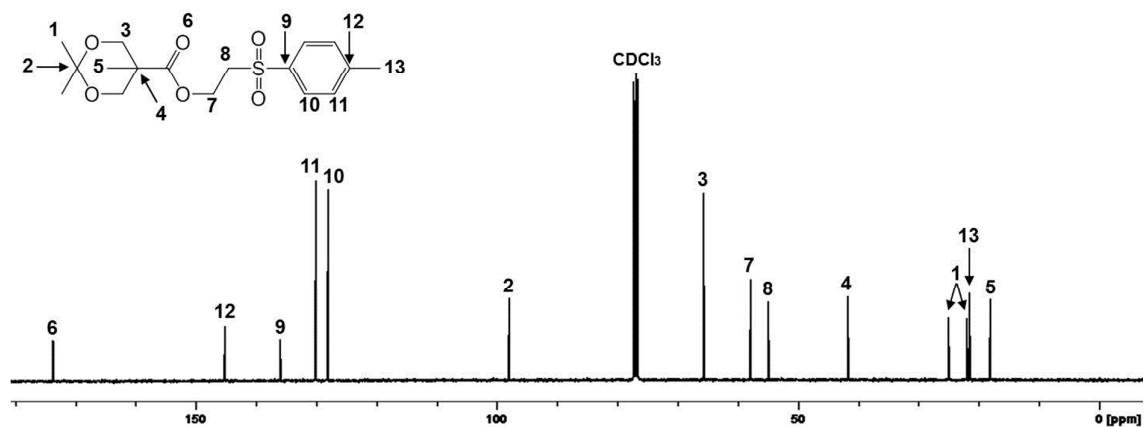
Figure S6. ^{13}C NMR (100 MHz, CDCl$_3$) of **[Acet$_1$-G$_1$-TSe]**
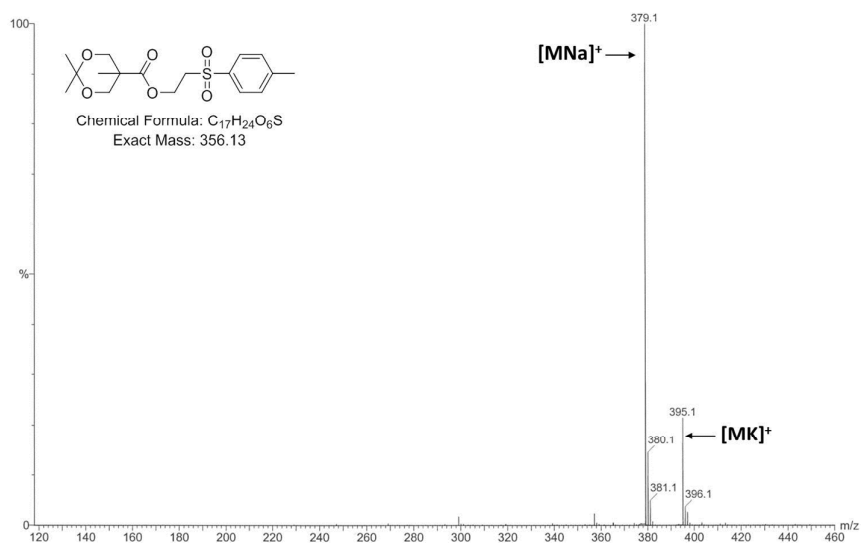
Figure S7. ESI MS (MeOH) of [Acet$_1$-G$_1$-TSe]
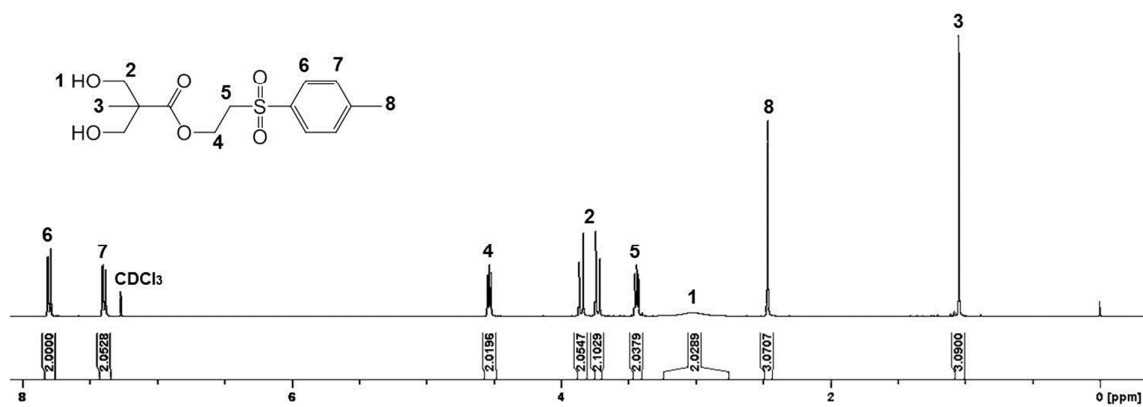
Figure S8. ^{1}H NMR (400 MHz, CDCl$_3$) of [(OH)$_2$-G$_1$-TSe]
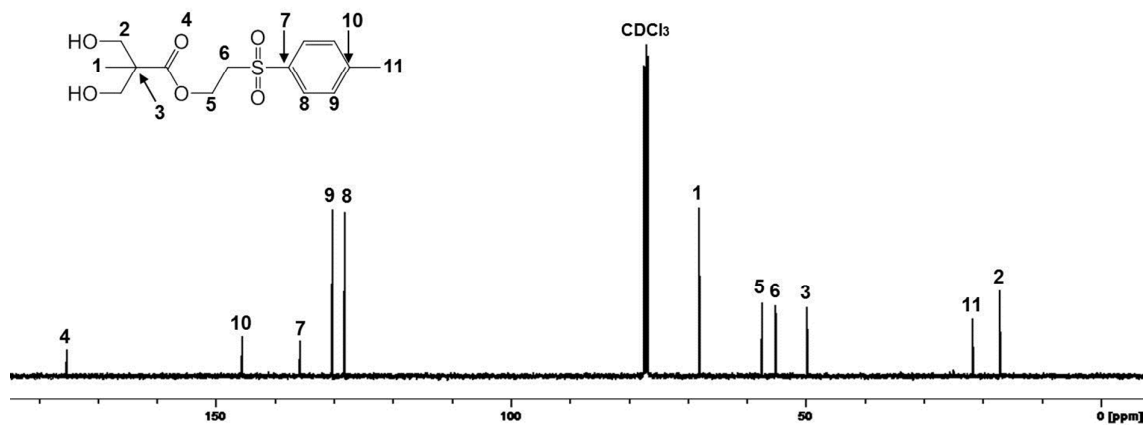
Figure S9. ^{13}C NMR (100 MHz, CDCl$_3$) of [(OH)$_2$-G$_1$-TSe]
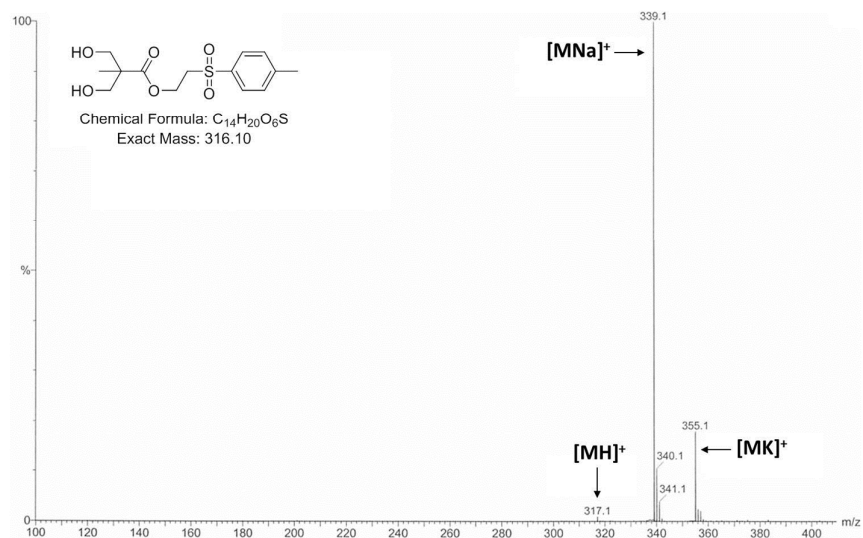
Figure S10. ESI MS (MeOH) of **[(OH)₂-G₁-TSe]**
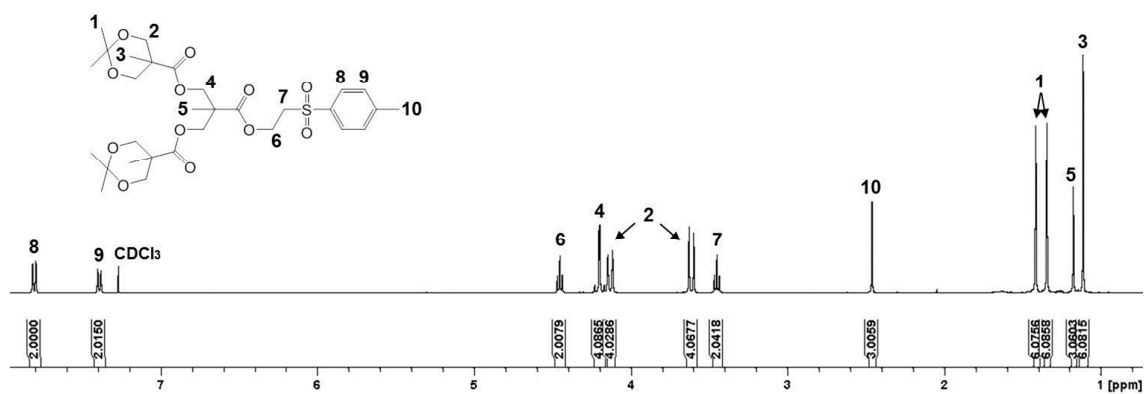
Figure S11. ¹H NMR (400 MHz, CDCl₃) of **[Acet₂-G₂-TSe]**
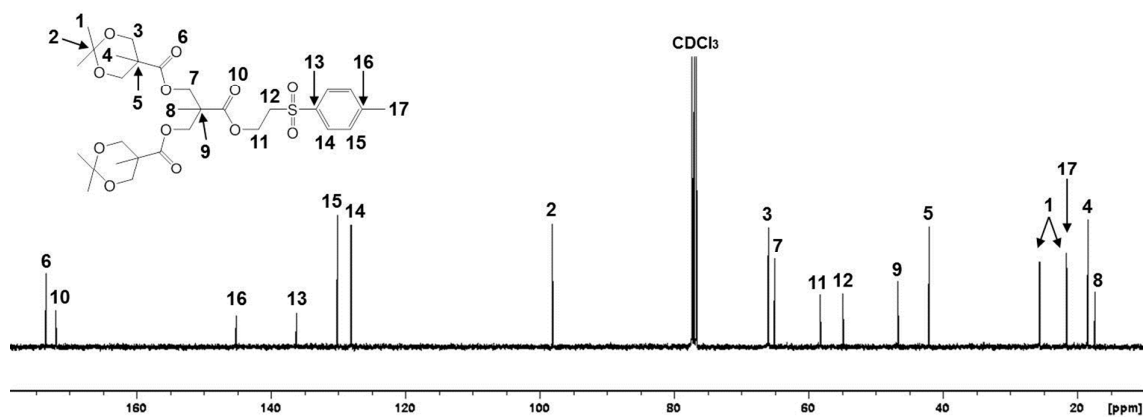
Figure S12. ¹³C NMR (100 MHz, CDCl₃) of **[Acet₂-G₂-TSe]**
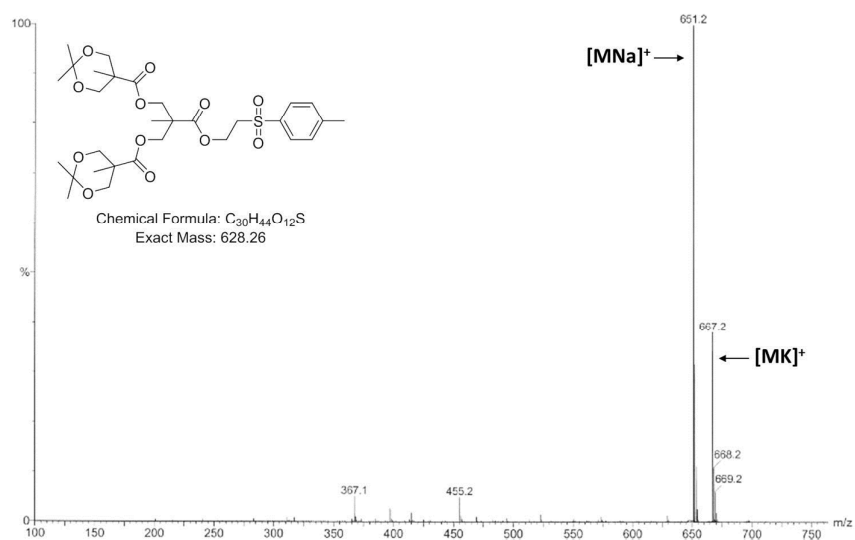
Figure S13. ESI MS (MeOH) of [Acet$_2$-G$_2$-TSe]
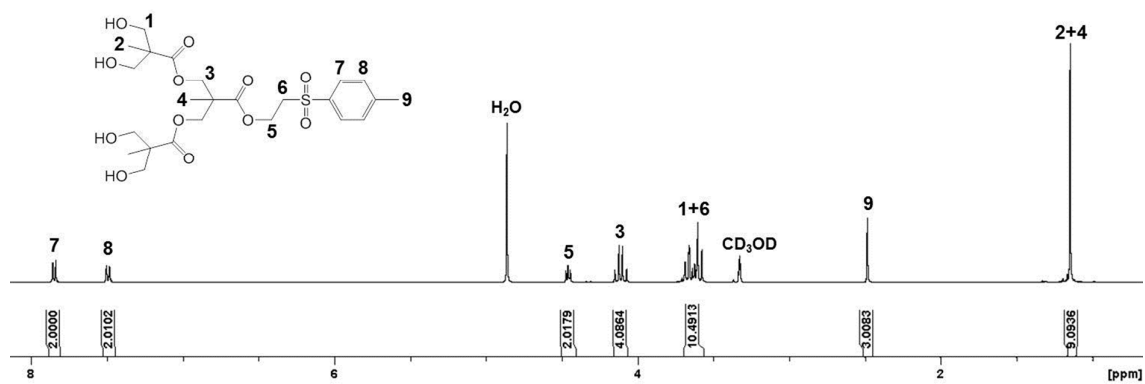
Figure S14. ^{1}H NMR (400 MHz, CD$_3$OD) of [(OH)$_4$-G$_2$-TSe]
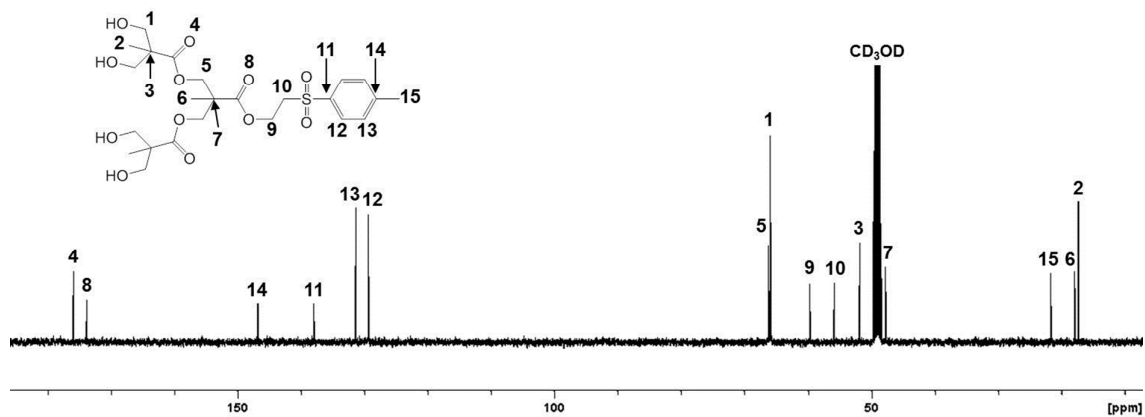
Figure S15. ^{13}C NMR (100 MHz, CD$_3$OD) of [(OH)$_4$-G$_2$-TSe]
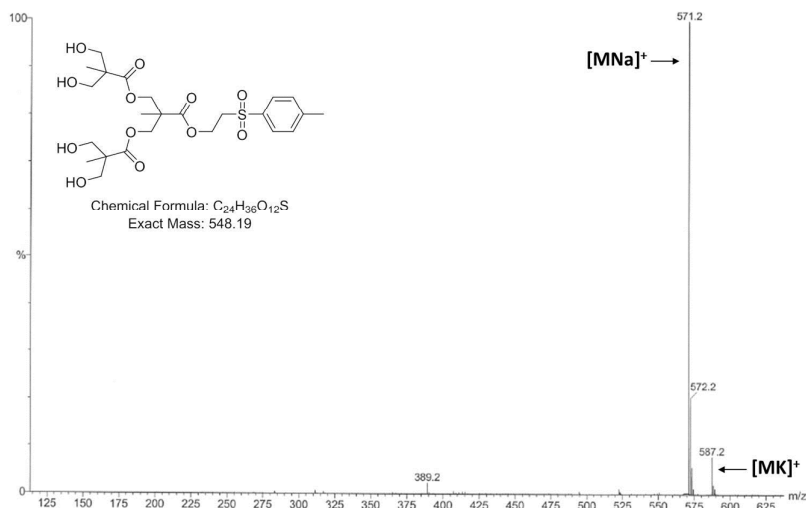
Figure S16. ESI MS (MeOH) of **[(OH)$_4$-G$_2$-TSe]**
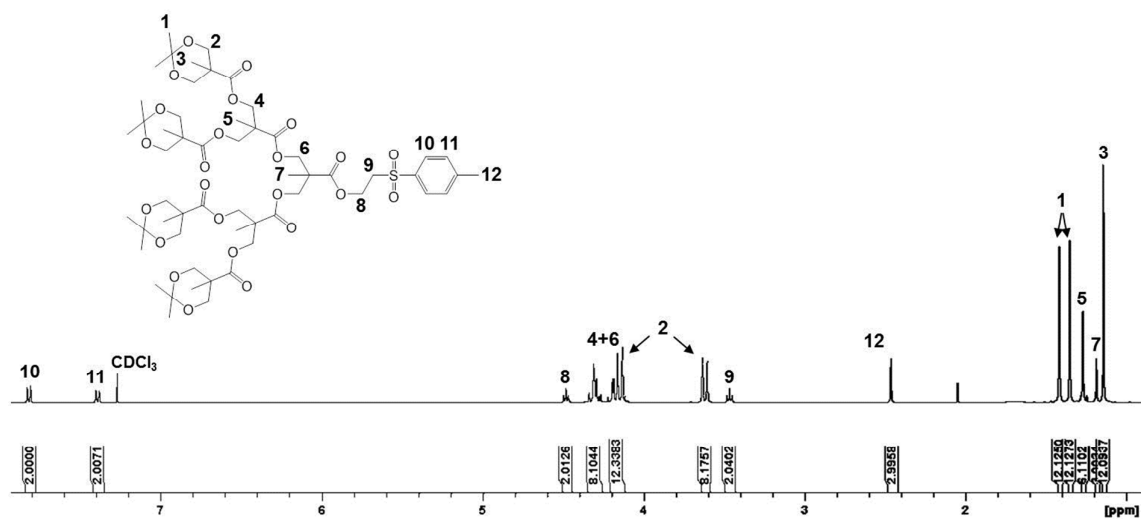
Figure S17. ^{1}H NMR (400 MHz, CDCl$_3$) of **[Acet$_4$-G$_3$-TSe]**
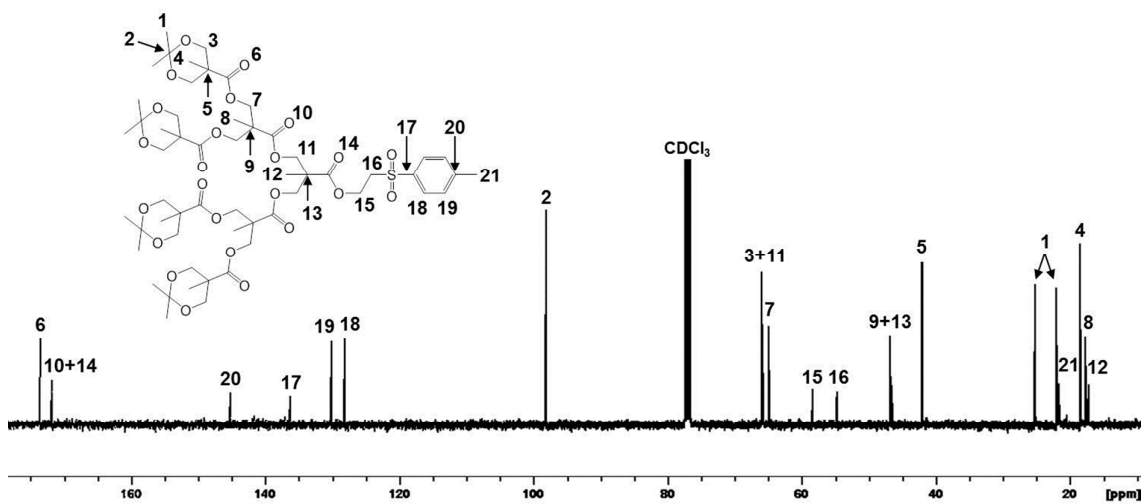
Figure S18. ^{13}C NMR (100 MHz, CDCl$_3$) of **[Acet$_4$-G$_3$-TSe]**
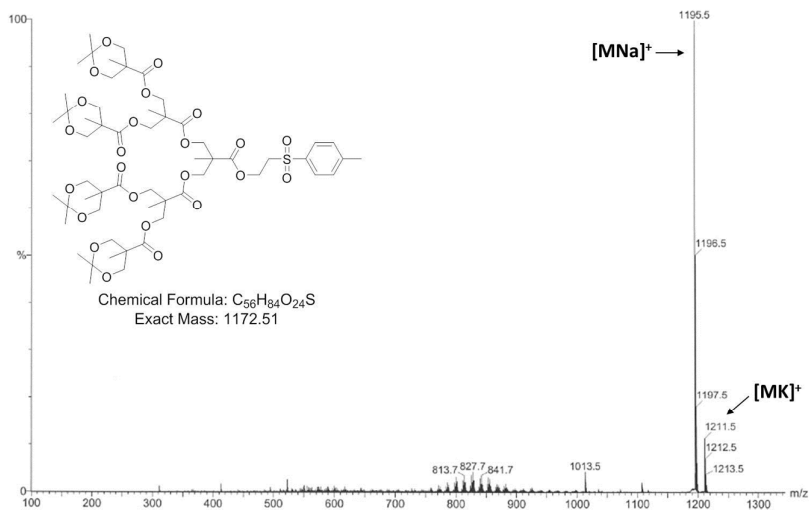
Figure S19. ESI MS (MeOH) of **[Acet₄-G₃-TSe]**
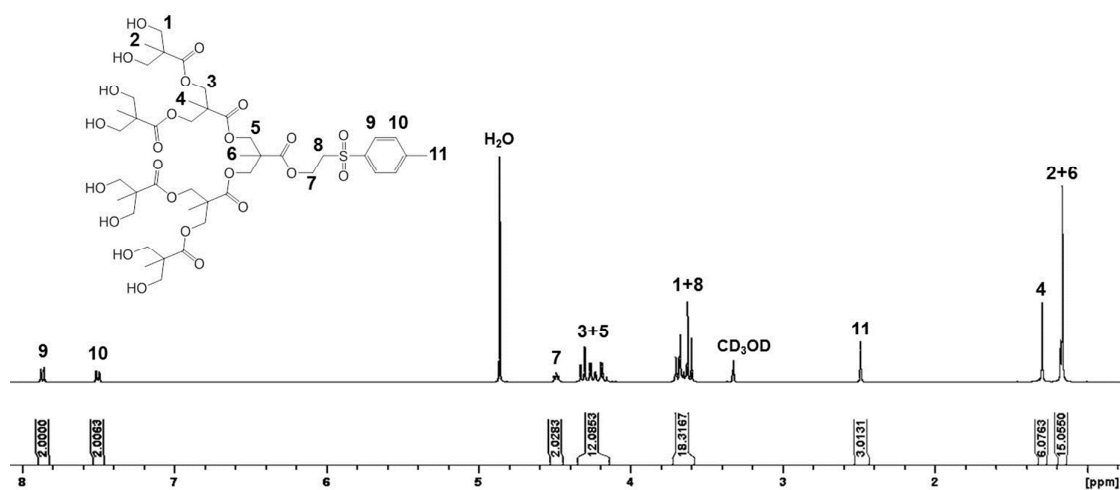
Figure S20. ¹H NMR (400 MHz, CD₃OD) of **[(OH)₈-G₃-TSe]**
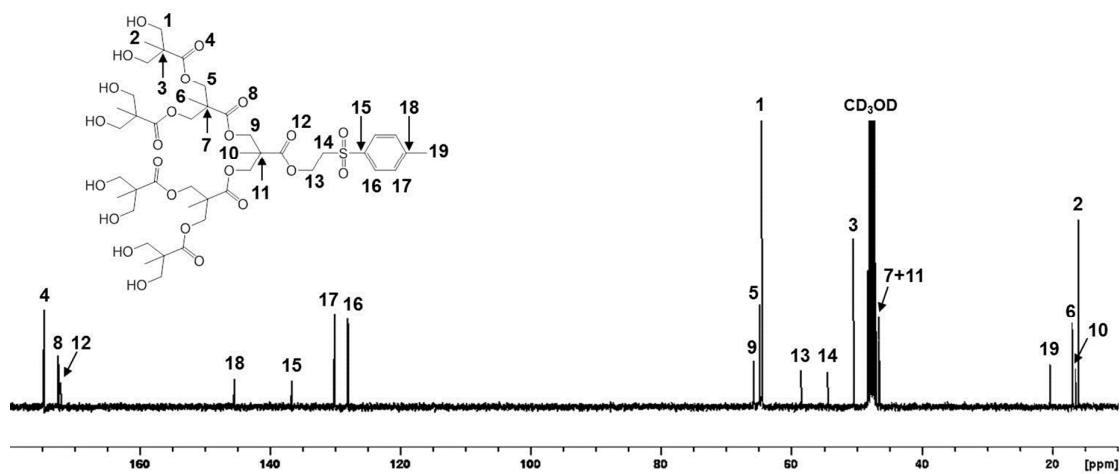
Figure S21. ¹³C NMR (100 MHz, CD₃OD) of **[(OH)₈-G₃-TSe]**
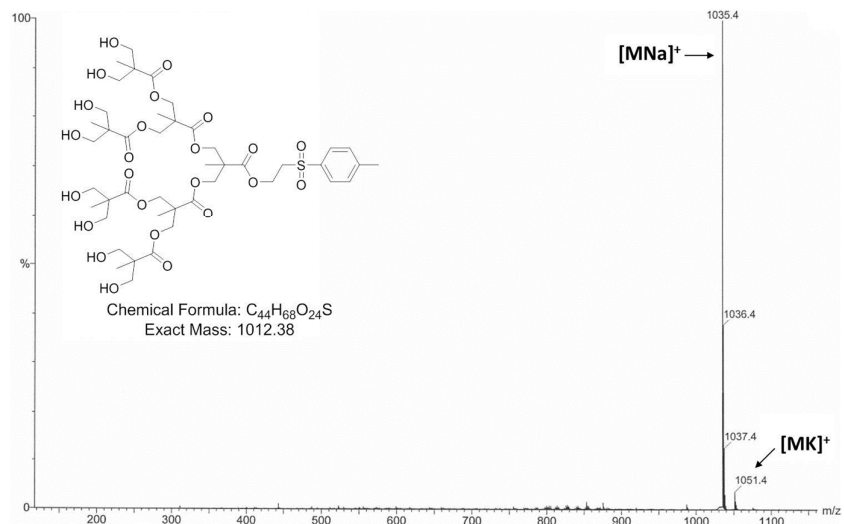
Figure S22. ESI MS (MeOH) of **[(OH)$_8$-G$_3$-TSe]**
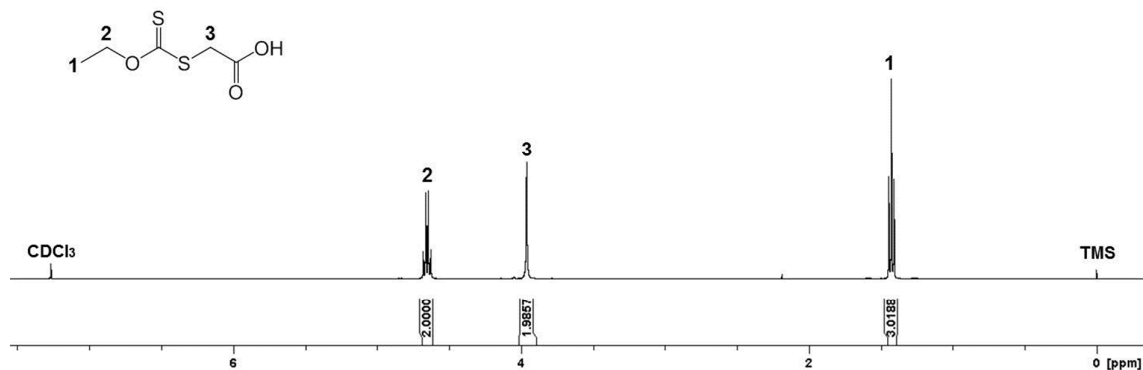
Figure S23. ^{1}H NMR (400 MHz, CDCl$_3$) of **2-((ethoxycarbonothioyl)thio)acetic acid [Xan-COOH]**
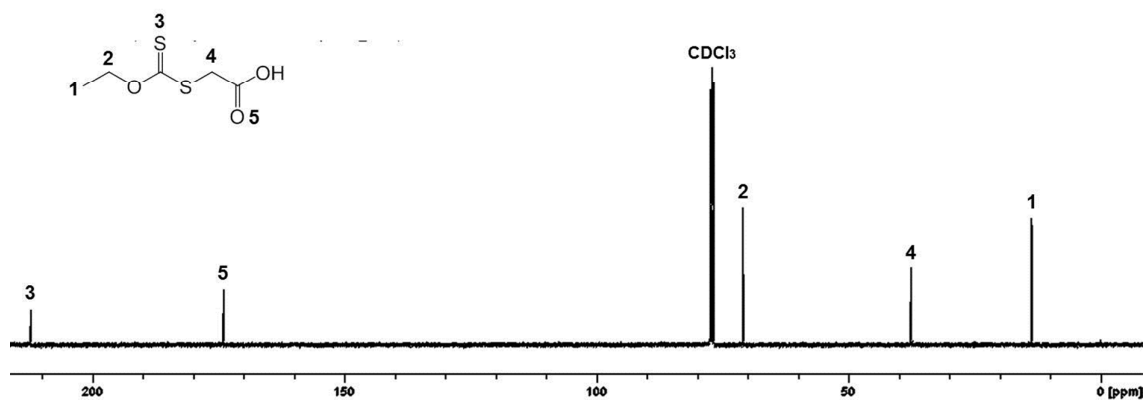
Figure S24. ^{13}C NMR (100 MHz, CDCl$_3$) of **2-((Ethoxycarbonothioyl)thio)acetic acid, [Xan-COOH]**

Figure S25. ^{1}H NMR (400 MHz, CDCl$_3$) of **2-((Ethoxycarbonothioyl)thio)acetic anhydride, [Xan-Anhy]**

Figure S26. ^{13}C NMR (100 MHz, CDCl$_3$) of **2-((Ethoxycarbonothioyl)thio)acetic anhydride, [Xan-Anhy]**

Figure S27. ^{1}H NMR (400 MHz, CDCl$_3$) of **[Xan$_8$-G$_3$-TSe]**
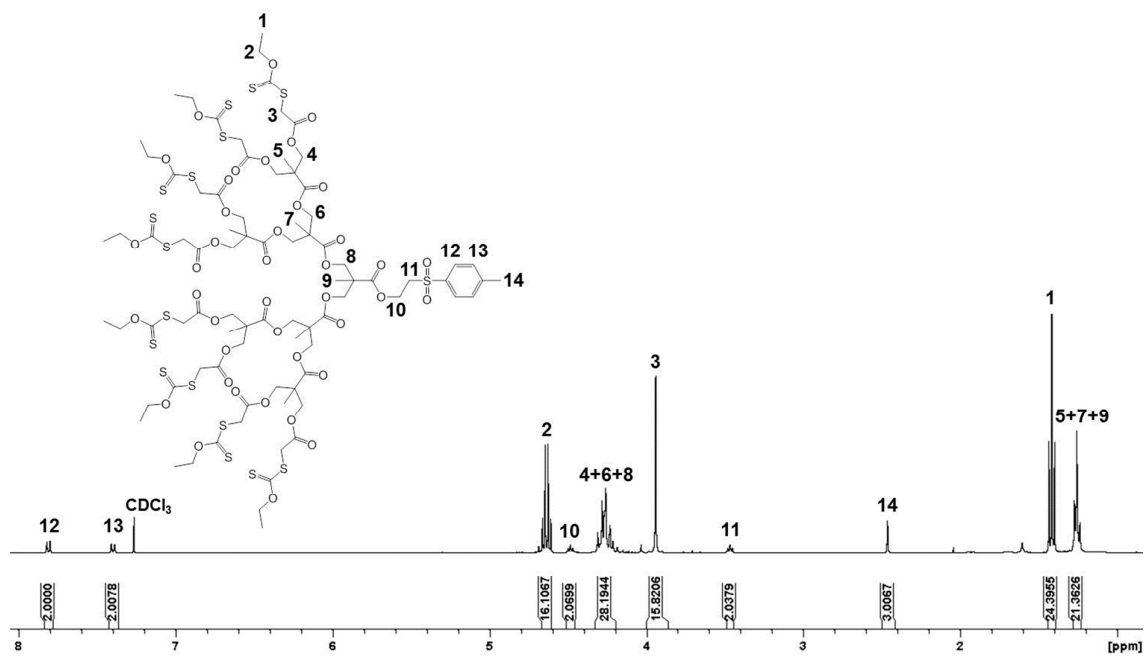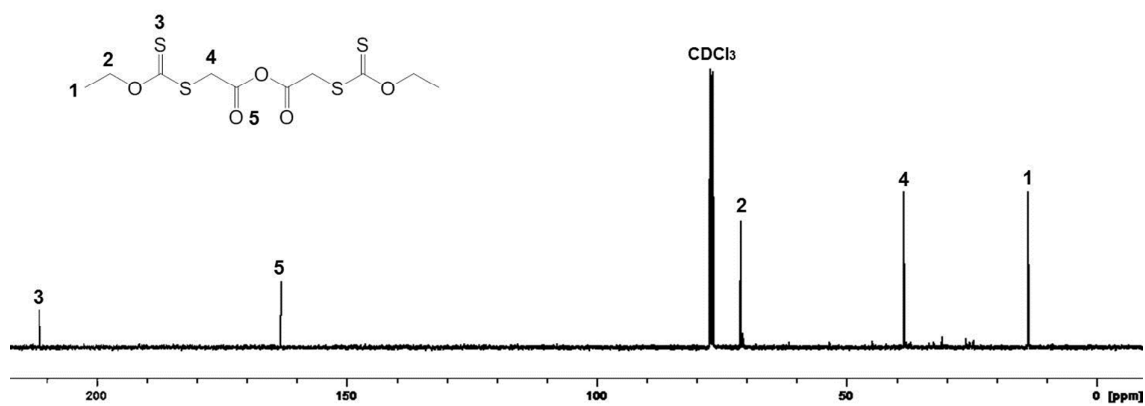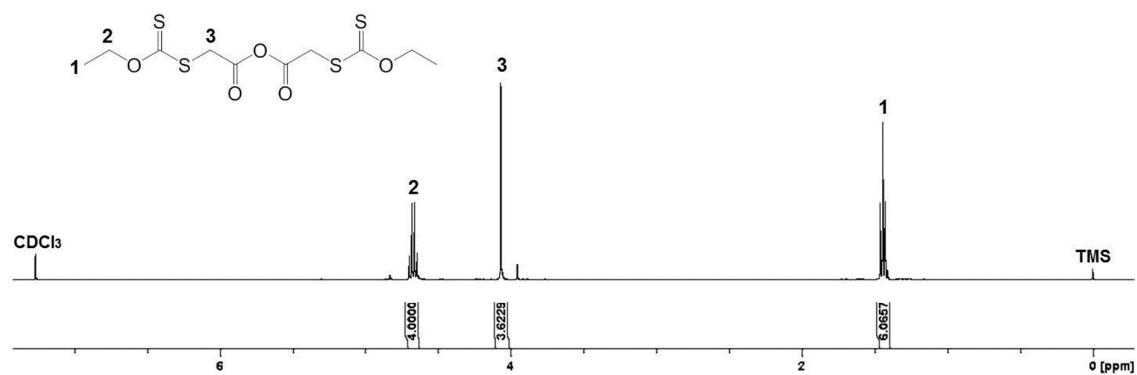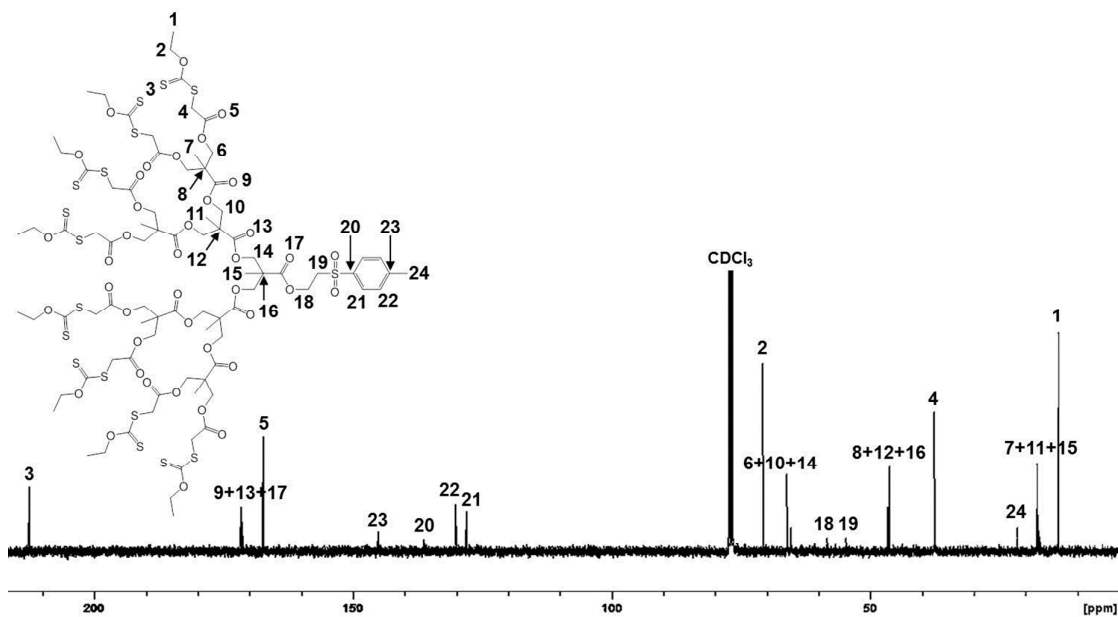
Figure S28. ^{13}C NMR (100 MHz, CDCl$_3$) of [**Xan$_8$-G$_3$-TSe**]
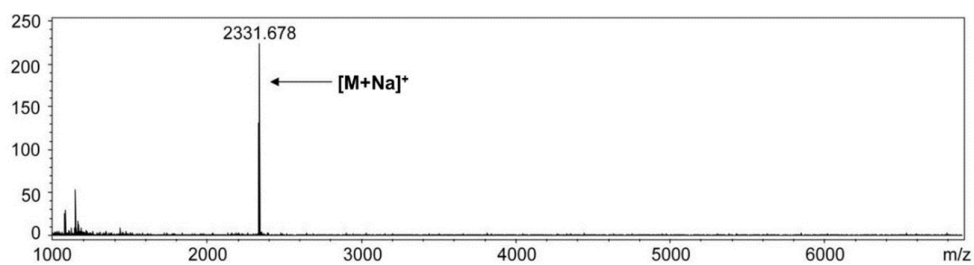
Figure S29. MALDI-TOF analysis of [**Xan$_8$-G$_3$-TSe**]
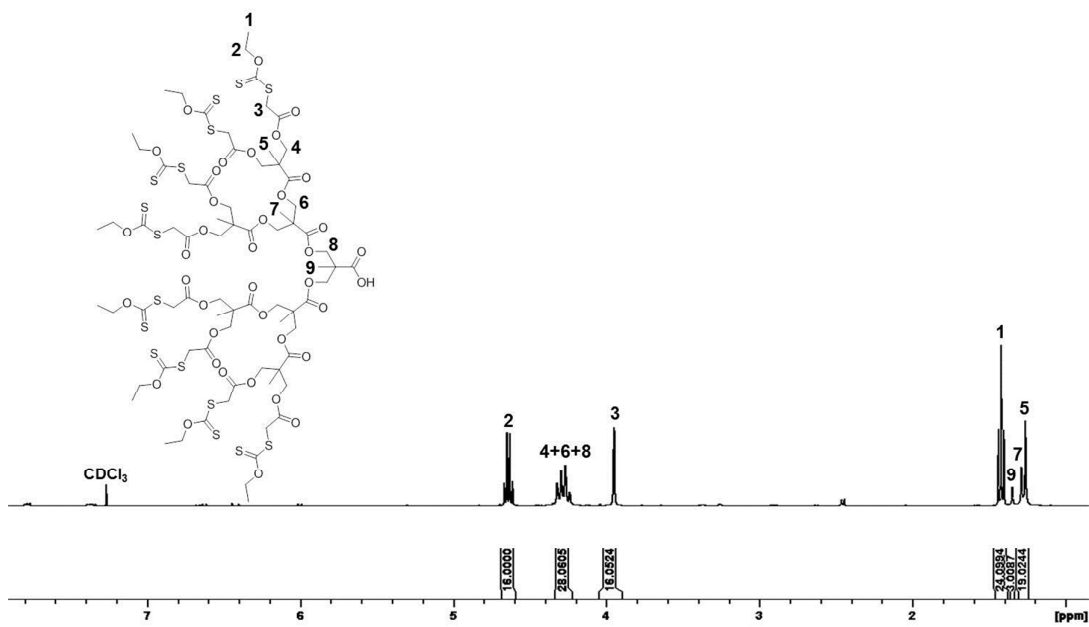
Figure S30. ^{1}H NMR (400 MHz, CDCl$_3$) of [**Xan$_8$-G$_3$-COOH**]
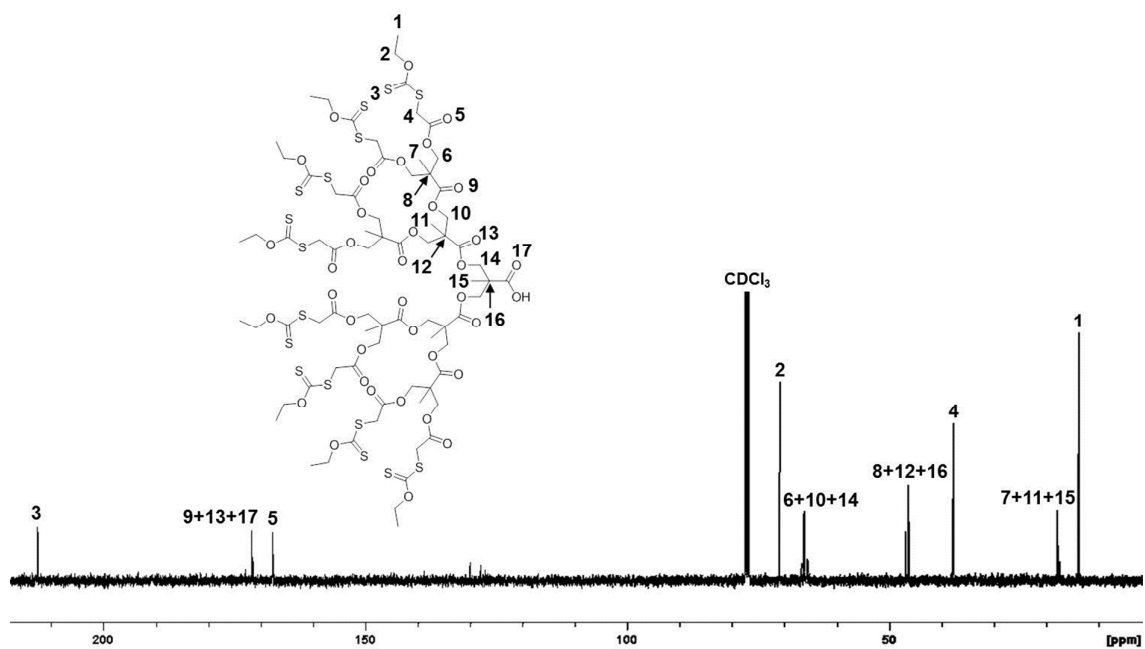
Figure S31. ^{13}C NMR (100 MHz, CDCl$_3$) of **[Xan$_8$-G$_3$-COOH]**
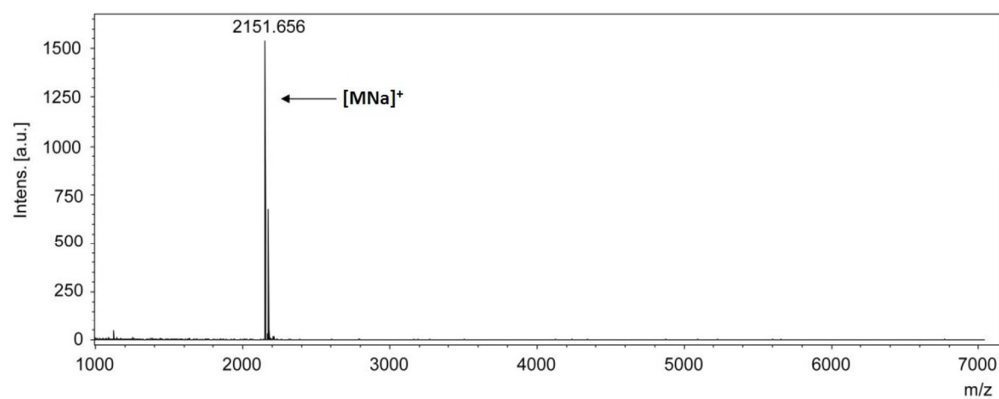
Figure S32. MALDI-TOF analysis of **[Xan$_8$-G$_3$-COOH]**
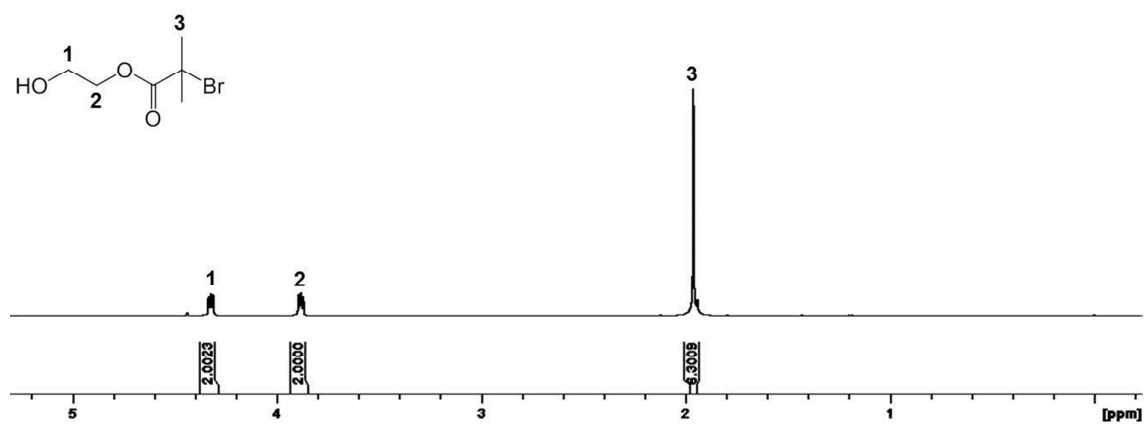
Figure S33. ^{1}H NMR (400 MHz, CDCl$_3$) of **[HEBiB]**
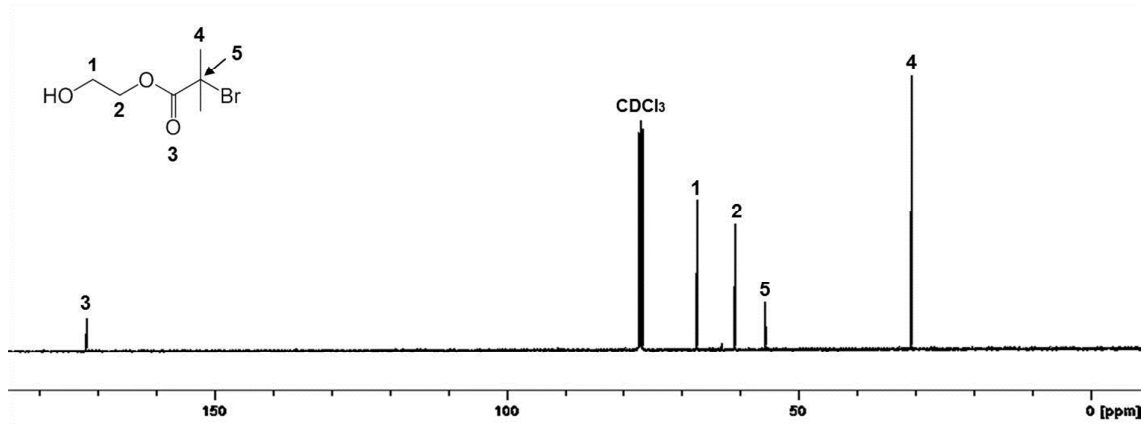
Figure S34. ^{13}C NMR (100 MHz, CDCl$_3$) of **[HEBiB]**
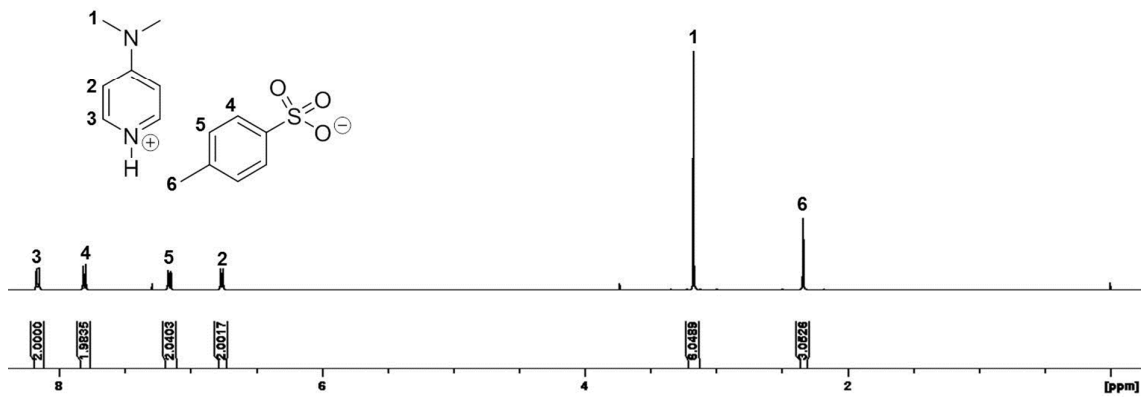
Figure S35. ^{1}H NMR (400 MHz, CDCl$_3$) of **DPTS**
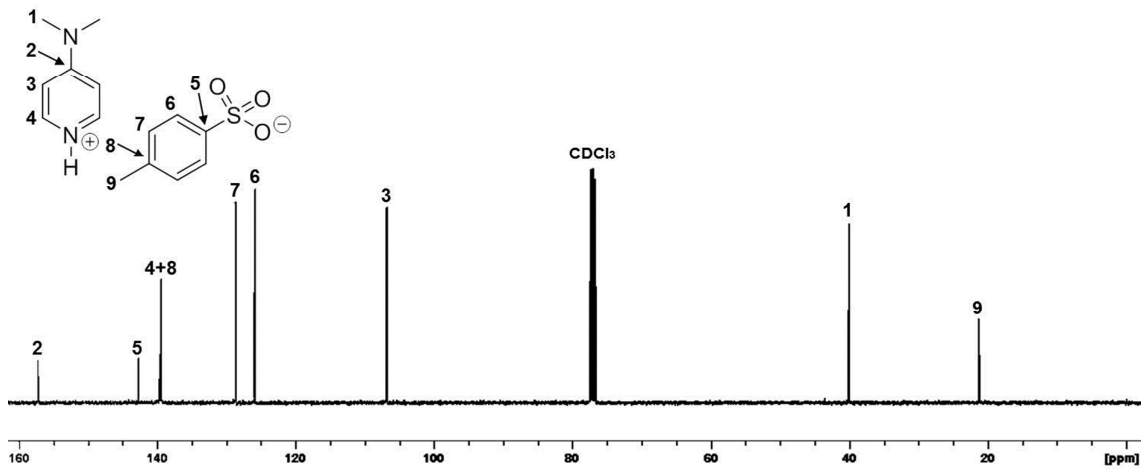
Figure S36. ^{13}C NMR (100 MHz, CDCl$_3$) of **DPTS**
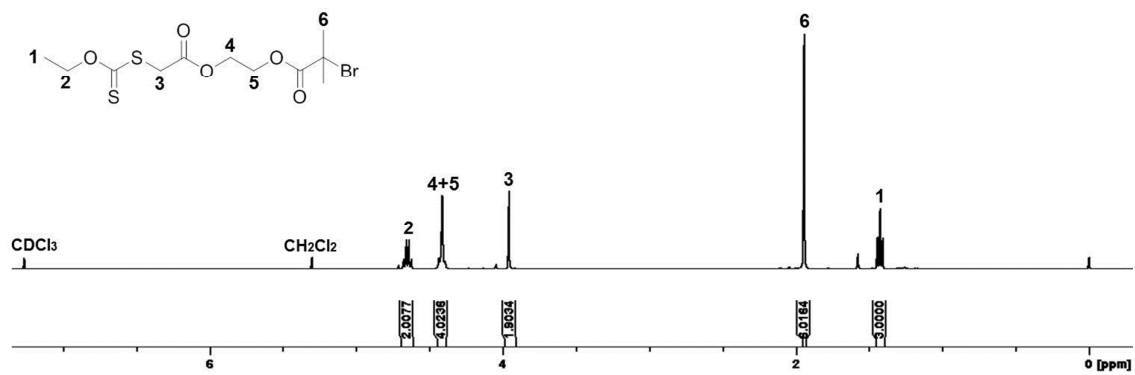
Figure S37. ^{1}H NMR (400 MHz, CDCl$_3$) of **[Xan$_1$-G$_0$-BiB]**
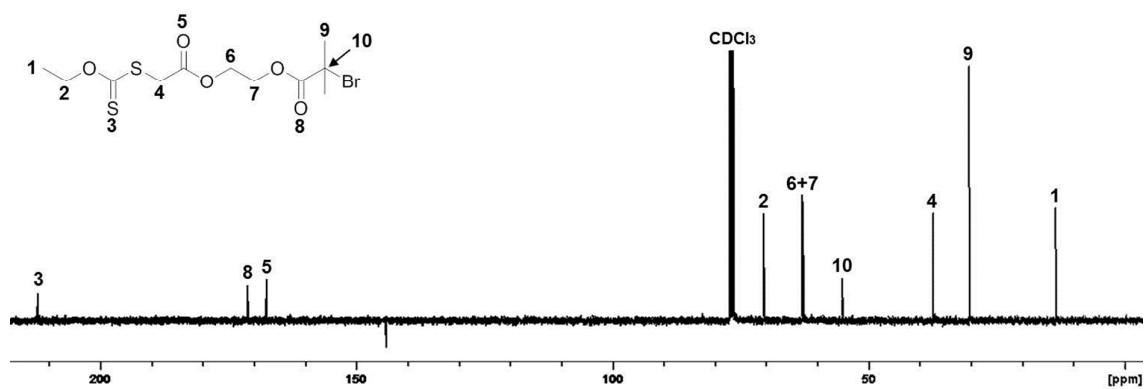
Figure S38. ^{13}C NMR (100 MHz, CDCl$_3$) of **[Xan$_1$-G$_0$-BiB]**
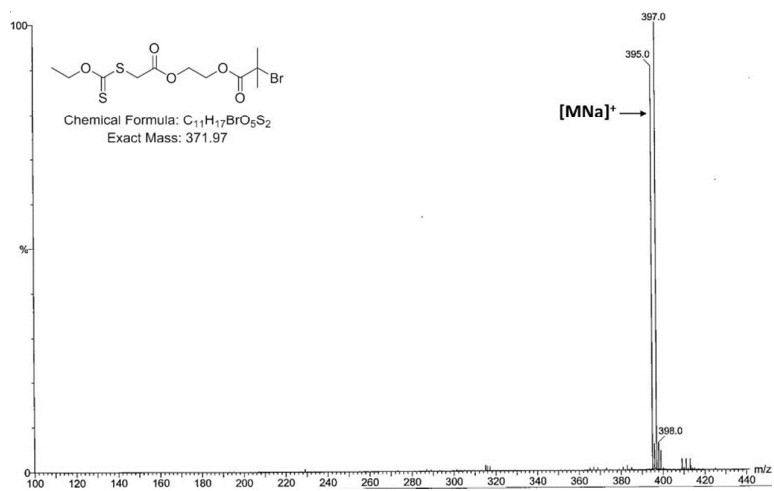
Figure S39. ESI-MS (MeOH) of **[Xan$_1$-G$_0$-BiB]**
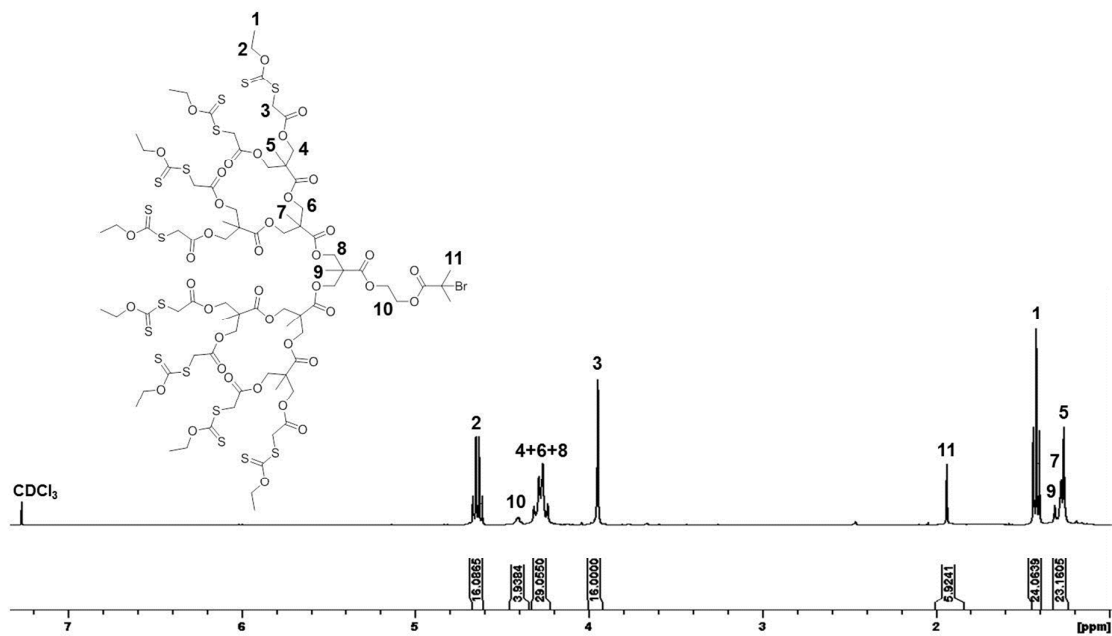
Figure S40. ^{1}H NMR (400 MHz, CDCl$_3$) of **[Xan$_8$-G$_3$-BiB]**
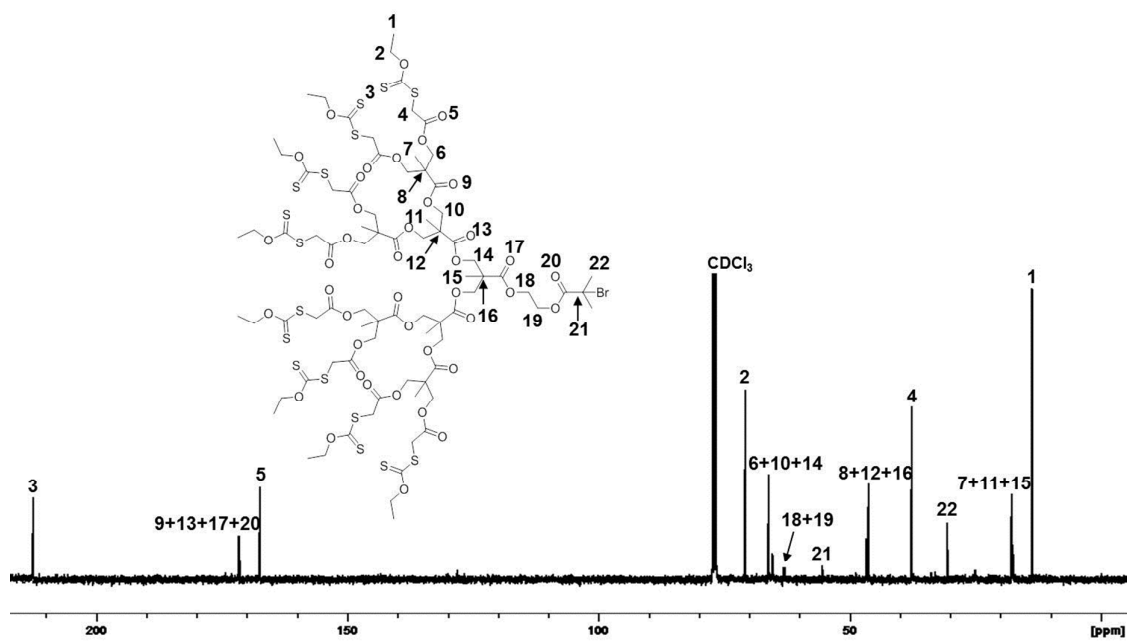
Figure S41. ^{13}C NMR (100 MHz, CDCl$_3$) of **[Xan$_8$-G$_3$-BiB]**
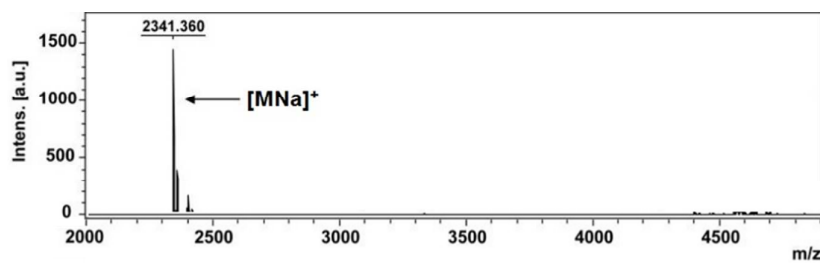
Figure S42. MALDI-TOF analysis of **[Xan$_8$-G$_3$-BiB]**
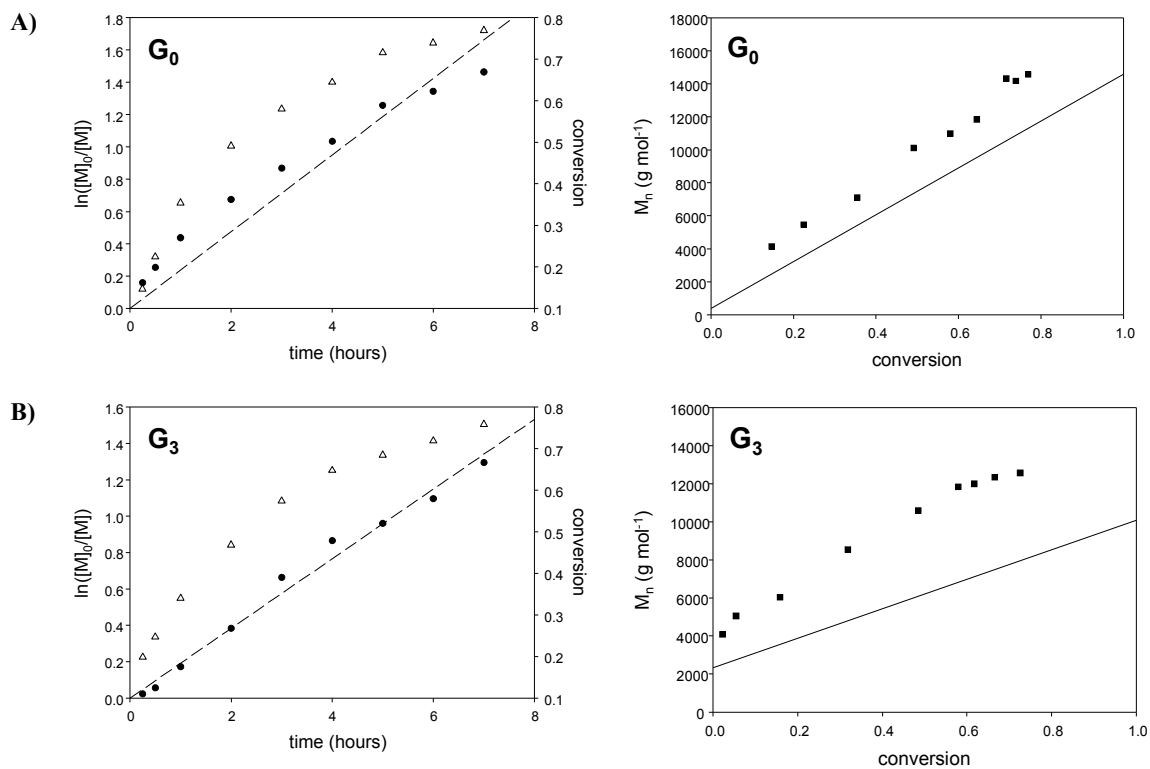
Figure S43. Kinetic studies of the ATRP of *n*-BuMA: A) **G$_0$-p(*n*-BuMA$_{100}$)**; and B) **G$_3$-p(*n*-BuMA$_{50}$)**. Conversion *vs*. time (open triangles) with corresponding semi-logarithmic plots (closed black circles); dashed line represents linear regression of semi-logarithmic plot. M$_n$ *vs*. conversion (closed black squares) and theoretical M$_n$ *vs*. conversion (solid line).
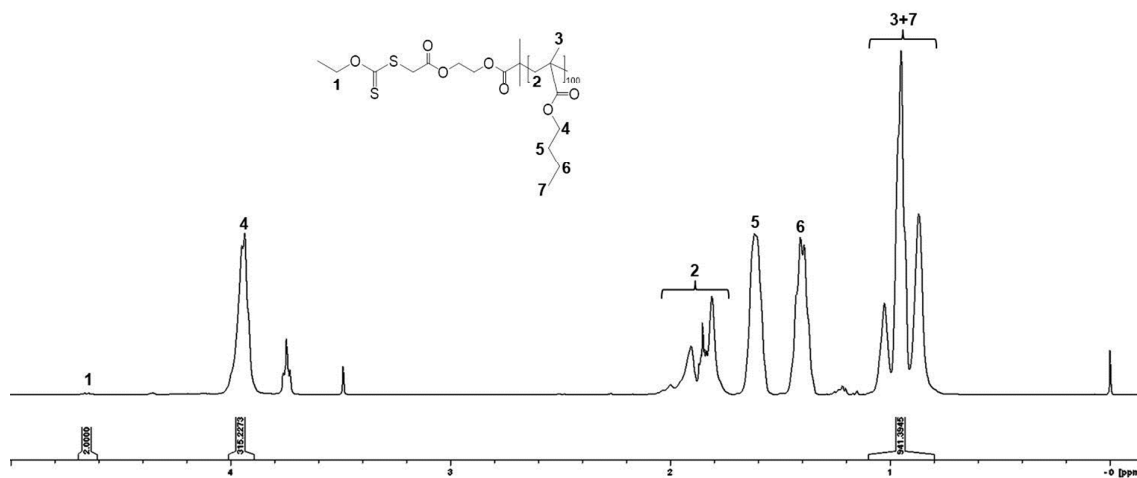
Figure S44. ^{1}H NMR (400MHz, CDCl$_3$) of **G$_0$-p(*n*-BuMA)$_{100}$**

Figure S45. ^{1}H NMR (400MHz, CDCl$_3$) of **G$_3$-p(*n*-BuMA)$_{100}$**

Figure S46. ^{1}H NMR (400 MHz, D$_2$O) of **[PEG$_{45}$-BiB]**

Figure S47. ^{13}C NMR (100 MHz, CDCl$_3$) of **[PEG$_{45}$-BiB]**
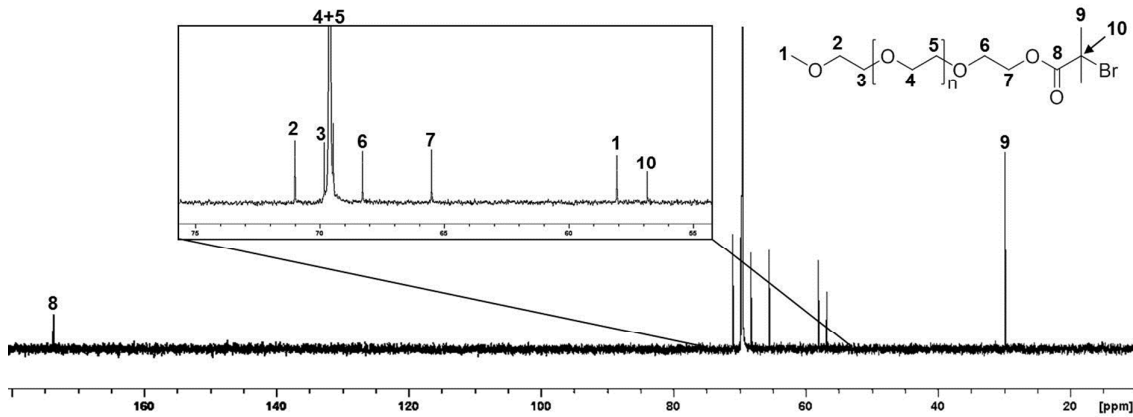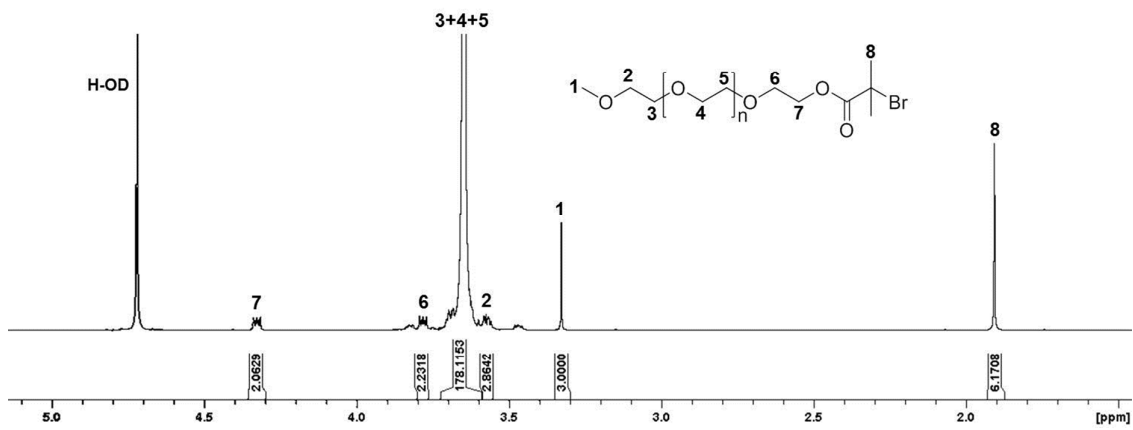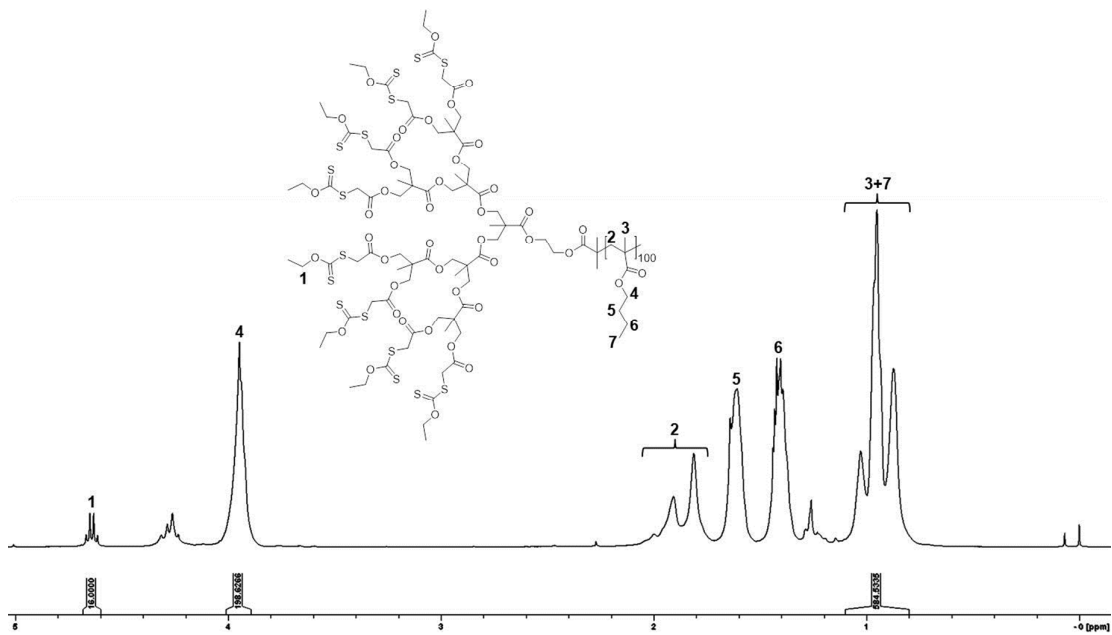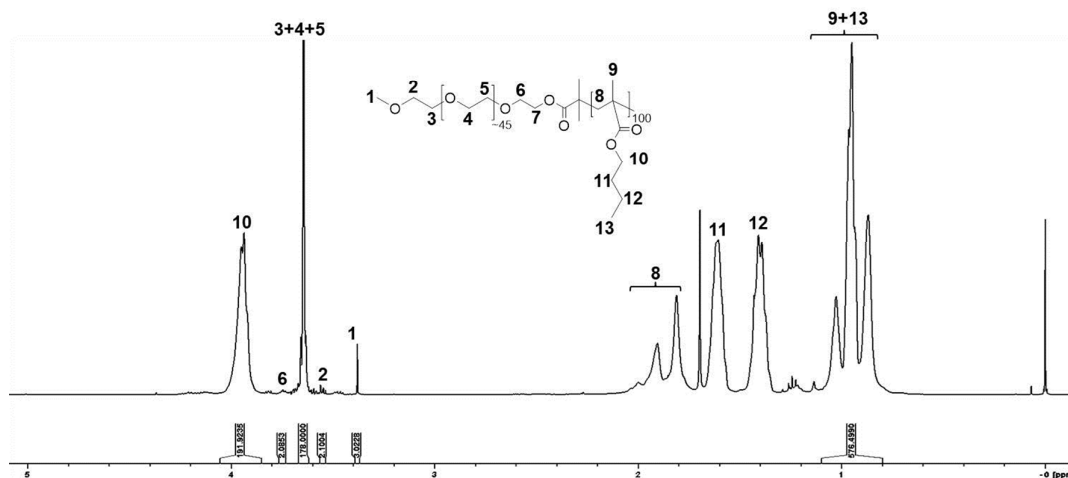
Figure S48. ^{1}H NMR (400MHz, CDCl$_3$) of **p(PEG$_{45}$-*b*-*n*-BuMA$_{100}$)**
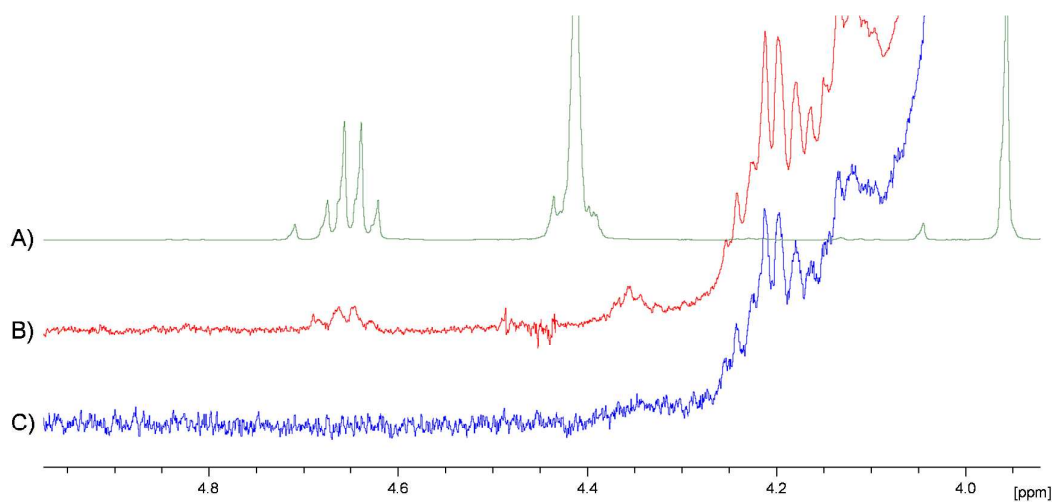
Figure S49. ^{1}H NMR (400MHz, CDCl$_3$) of: A) **[Xan$_1$-G$_0$-BiB]**; B) **[(G$_0$)$_{0.1}$-(PEG$_{45}$)$_{0.9}$]-p(*n*-BuMA$_{100}$-*co*-EGDMA$_{0.8}$)**; and C) deprotected **[(G$_0$)$_{0.1}$-(PEG$_{45}$)$_{0.9}$]-p(*n*-BuMA$_{100}$-*co*-EGDMA$_{0.8}$)**
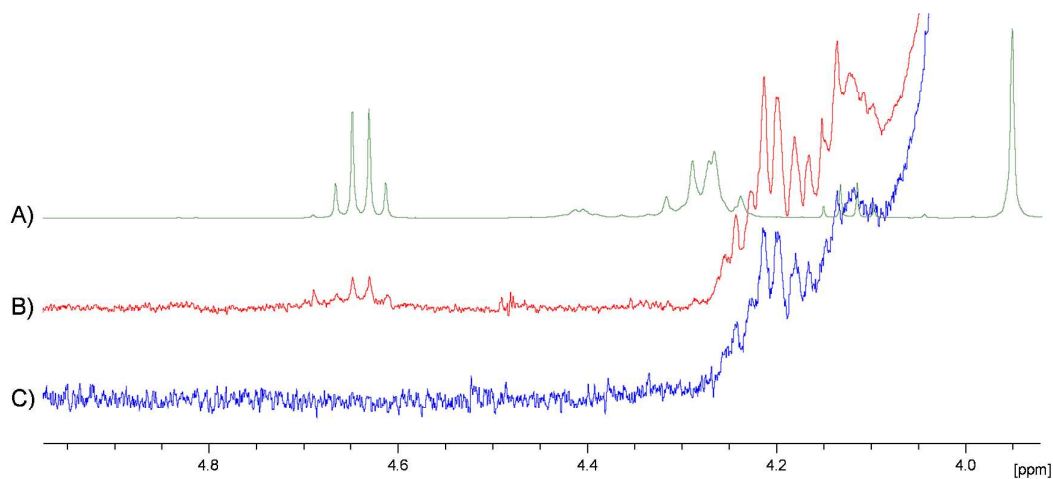
Figure S50. ^{1}H NMR (400MHz, CDCl$_3$) of: A) **[Xan$_8$-G$_3$-BiB]**; B) **[(G$_3$)$_{0.014}$-(PEG$_{45}$)$_{0.986}$]-p(*n*-BuMA$_{100}$-*co*-EGDMA$_{0.8}$)**; and C) deprotected **[(G$_3$)$_{0.014}$-(PEG$_{45}$)$_{0.986}$]-p(*n*-BuMA$_{100}$-*co*-EGDMA$_{0.8}$)**
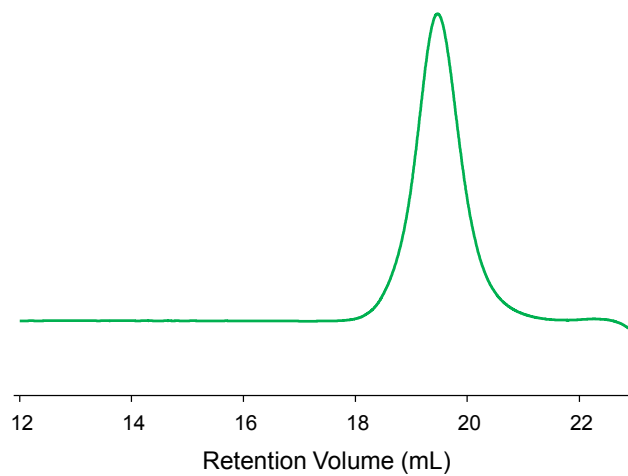
Figure S51. SEC chromatogram (RI) of linear polymer G_0-p(n-BuMA)$_{100}$
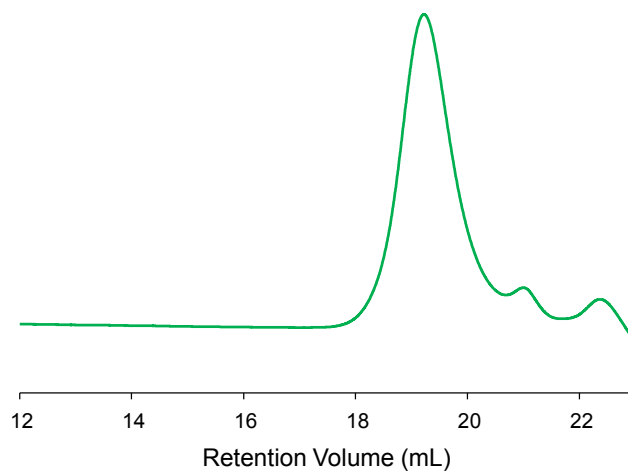
Figure S52. SEC chromatogram (RI) of linear dendritic hybrid polymer G_3-p(n-BuMA)$_{100}$
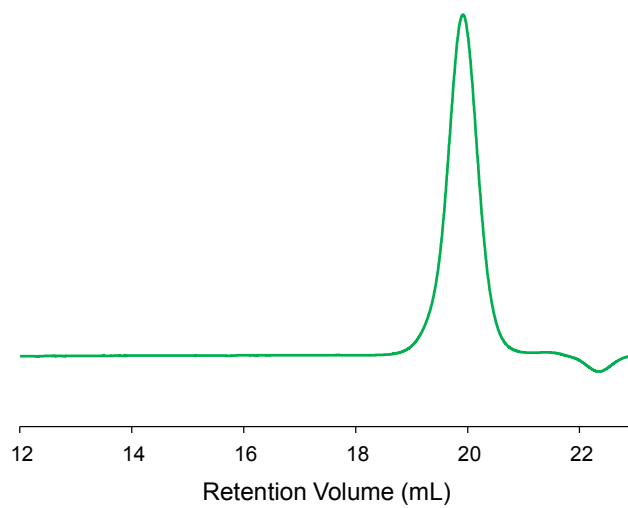
Figure S53. SEC chromatogram (RI) of linear block copolymer p(PEG$_{45}$-b-n-BuMA$_{100}$)
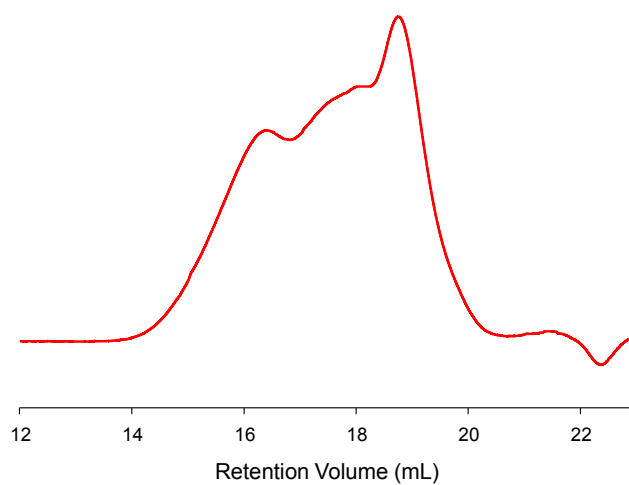
Figure S54. SEC chromatogram (RI) of HPD $[(G_0)_{0.01}\text{-}(PEG_{45})_{0.99}]\text{-}p(n\text{-}BuMA_{100}\text{-}co\text{-}EGDMA_{0.8})$
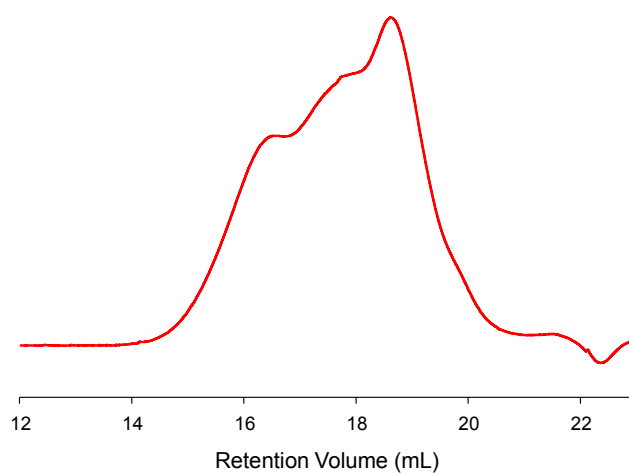
Figure S55. SEC chromatogram (RI) of HPD $[(G_0)_{0.075}\text{-}(PEG_{45})_{0.925}]\text{-}p(n\text{-}BuMA_{100}\text{-}co\text{-}EGDMA_{0.8})$
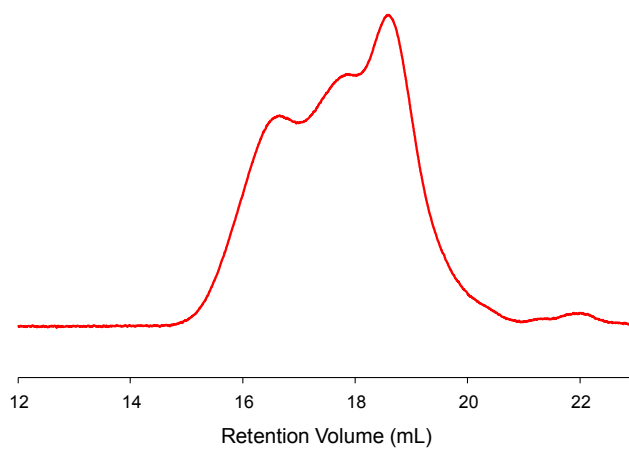
Figure S56. SEC chromatogram (RI) of HPD $[(G_0)_{0.1}\text{-}(PEG_{45})_{0.9}]\text{-}p(n\text{-}BuMA_{100}\text{-}co\text{-}EGDMA_{0.8})$
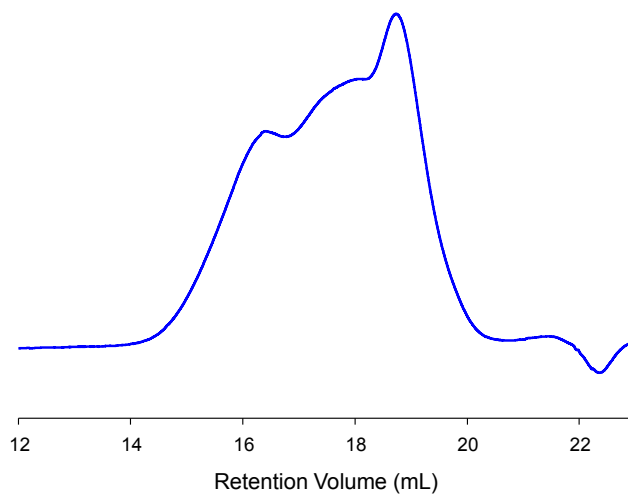
Figure S57. SEC chromatogram (RI) of HPD **[(G$_3$)$_{0.01}$-(PEG$_{45}$)$_{0.99}$]-p(n-BuMA$_{100}$-co-EGDMA$_{0.8}$)**
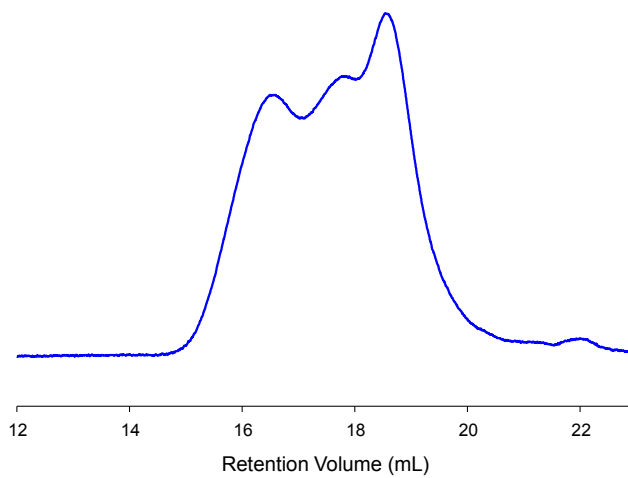
Figure S58. SEC chromatogram (RI) of HPD **[(G$_3$)$_{0.014}$-(PEG$_{45}$)$_{0.986}$]-p(n-BuMA$_{100}$-co-EGDMA$_{0.8}$)**
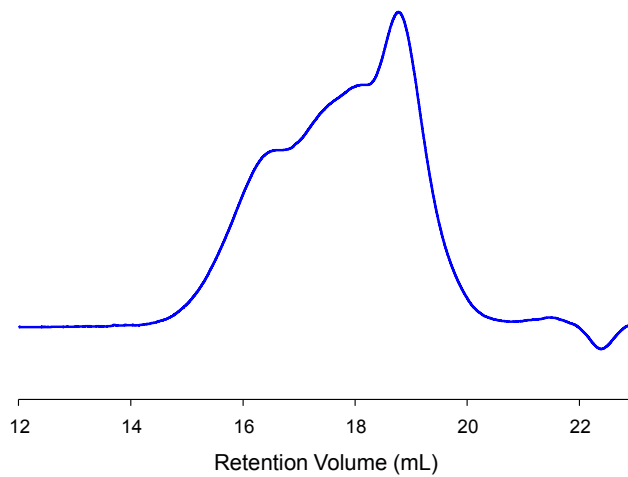
Figure S59. SEC chromatogram (RI) of HPD **[(G$_3$)$_{0.05}$-(PEG$_{45}$)$_{0.95}$]-p(n-BuMA$_{100}$-co-EGDMA$_{0.8}$)**
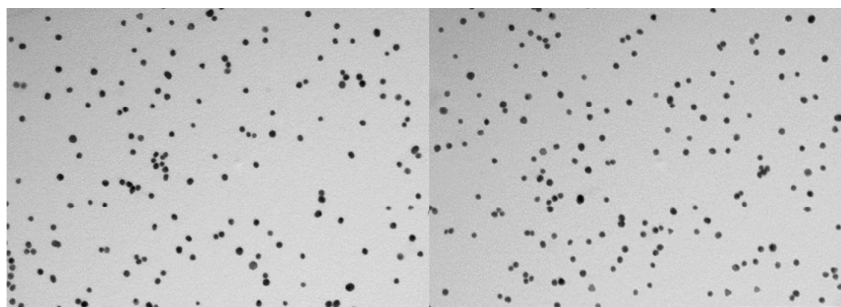
Figure S60. TEM images of 4 nm GNPs synthesised by the Inverse Turkevich method
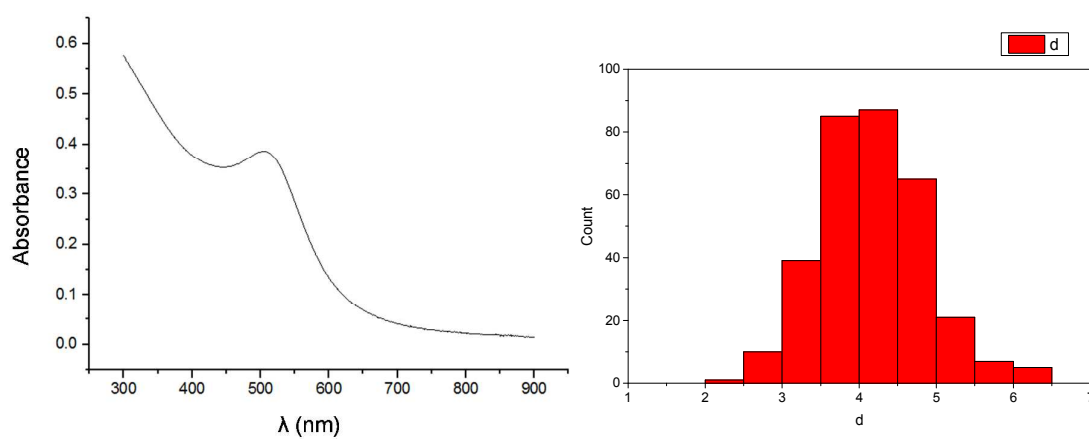
	N total	Mean	Standard Deviation	Sum	Minimum	Median	Maximum
d	323	4.13583	0.77112	1335.87358	0.51586	4.07093	6.30369

Figure S61. Size determination of GNPs by UV-Vis spectroscopy

Polymer Chemistry

Table S1. DLS data for: $[(G_0)_x\text{-}(PEG_{45})_y]\text{-}p(n\text{-}BuMA_{100}\text{-}co\text{-}EGDMA_{0.8})$; **a** (x = 0.01, y = 0.99); **b** (x = 0.075, y = 0.925); **c** (x = 0.1, y = 0.9); and $[(G_3)_x\text{-}(PEG_{45})_y]\text{-}p(n\text{-}BuMA_{100}\text{-}co\text{-}EGDMA_{0.8})$; **d** (x = 0.01, y = 0.99); **e** (x = 0.014, y = 0.986); **f** (x = 0.05, y = 0.95) nanoprecipitates 1 year stability studies at ambient temperature with coordinated 4 nm GNPs

| Material | Initiator (%) | | | | Original | | | | 1 year | |
	G_0	G_3	PEG_{45}	GNPs	D_z	PdI	D_z	PdI	polymer nanoparticle suspension	polymer nanoparticle suspension + 4 nm GNPs
a	1	0	99	-	53	0.128	56	0.101		
a	1	0	99	✓	60	0.230	55	0.078		
b	7.5	0	92.5	-	52	0.083	56	0.063		
b	7.5	0	92.5	✓	64	0.224	54	0.082		
c	10	0	90	-	65	0.097	65	0.100		
c	10	0	90	✓	74	0.235	61	0.134		
d	0	1	99	-	51	0.105	53	0.094		
d	0	1	99	✓	54	0.124	60	0.102		
e	0	1.4	98.6	-	61	0.141	62	0.107		
e	0	1.4	98.6	✓	66	0.190	78	0.167		
f	0	5	95	-	52	0.101	55	0.065		
f	0	5	95	✓	56	0.101	56	0.083		